

PRACTICAL IMPLEMENTATION OF ASSEMBLY PROCESSES FOR LOW-MELTING POINT SOLDER PASTES

Adam Murling, Miloš Lazić, Don Wood, and Brook Sandy-Smith
Indium Corporation
amurling@indium.com, mlazic@indium.com, bsandy@indium.com

Martin Anselm
Rochester Institute of Technology
mkamet@rit.edu

ABSTRACT

In the last three to five years, there has been a resurgence of interest in the use of low-melting point alloys for SMT applications. Typically the compositions are around the eutectic bismuth-tin alloy, perhaps with additions of other elements to increase the robustness of certain alloy properties. Now, there are several new products on the market and numerous ongoing reliability projects in industry consortia.

Alloy reliability is typically the main focus of the ongoing research, but this study will investigate the “process-ability” of these new materials and considerations to implement a new low-melting point solder paste assembly process. Data presented will compare the stencil printing performance of some of these materials to leading next-generation, Pb-free, no-clean materials. There will also be a discussion of reflow approaches for the best success.

Key Words: Low-temp solder, Bismuth, Indium, Reflow, Printability

INTRODUCTION

Bismuth-tin solder alloys have drawn interest for electronics applications for decades. The melting point around 140°C is very desirable because it allows for use of lower temp laminate materials and reduces thermal stress on sensitive components. Originally, it was considered a good alternative to wave soldering processes, bolstered by the intrinsic reliability of through-hole components.

Since 2006 and the implementation of the RoHS directive, the interest in bismuth-tin solder alloys has only increased as the industry has searched for Pb-free alternatives to the chosen standard, SAC305, which melts at considerably higher temperatures than the incumbent tin-lead alloys.

Now there are new drivers toward consideration of low-melting point alloys. Lower processing temperatures are tempting because they reduce process costs. Lower processing temperatures may also facilitate designs that would be challenging to assemble with tin-based alloys. Additionally, as component architectures get thinner, component manufacturers have explored the option to align the solder alloy melting point with the inflection point where component warpage is at its least.

These factors have driven renewed interest in bismuth-tin alloys and the development of new alloy options with improved mechanical properties. These new alloy options also include alloys composed of tin and indium, or bismuth-tin with minor elemental additions of silver, antimony, or nickel.

This paper will discuss the background and need for low-temperature solders and compare the processability of solder pastes with three novel alloys against the industry standard 57Bi/42Sn/1Ag.

BACKGROUND

The most noticeable difference in the performance of bismuth-tin alloys is the brittleness of the resulting solder joints. This eliminates bismuth-tin as an option for applications where drop shock reliability is critical. Other properties such as thermal cycling reliability and electrical/thermal performance are promising. Further alloy development has been focused on maximizing these forms of reliability to the result of a more robust low-melting point soldering solution.

In regards to thermal cycling, bismuth-tin alloys have a shorter life due to peak cycling temperatures in closer proximity to the lower melting point. This increases the challenge associated with such testing. When you couple this with a less-than optimal thermal conductivity rating, solder joint failure becomes a major

concern for reliability, especially for high current applications.

Early adopters of bismuth-tin alloys had to be very careful about interaction with Pb. If this alloy makes contact with any amount of lead, for example on component leads or board surface finishes, there is a phase formed which melts at a much lower temperature and will compromise the integrity of solder joints¹.

Reliability studies have shown that silver additions as little as 1% substantially increase the thermal conductivity, shear-strength, and tensile strength, while still providing a low-melting point alternative to Pb-based alloys. With 1% silver the resulting melting point is 138-140°C. Most early applications adopted this alloy because of the considerable benefits, without trade-offs.

Careful consideration must be used when choosing a flux vehicle for low-melting point solder pastes. The flux that is chosen must activate at a much lower temperature than standard fluxes due to the low-melting point. A majority of fluxes used in 63Sn/37Pb or SAC305 are not recommended for low-melting point alloys. In order to increase the reliability of the alloy and ensure a robust solder joint, the flux vehicle is imperative.

As technology advances, the performance requirements for low-temperature alternatives are becoming more demanding. Solder pastes developed in the early adoption of bismuth-tin eutectic alloy do not achieve printing and reflow performance to rival modern Pb-

free solder pastes. Recent studies² have focused on the reliability of newly developed alloys, but have overlooked the process-ability in solder paste form. Bulk properties of an alloy may be promising, but if a solder paste does not have excellent stencil printing, stability, and reflow performance, it will not be easily adopted.

EXPERIMENT

There were four solder pastes printed and tested: a bismuth containing baseline (57Bi 42Sn 1Ag), two novel bismuth-based alloys, and an indium-based alloy.

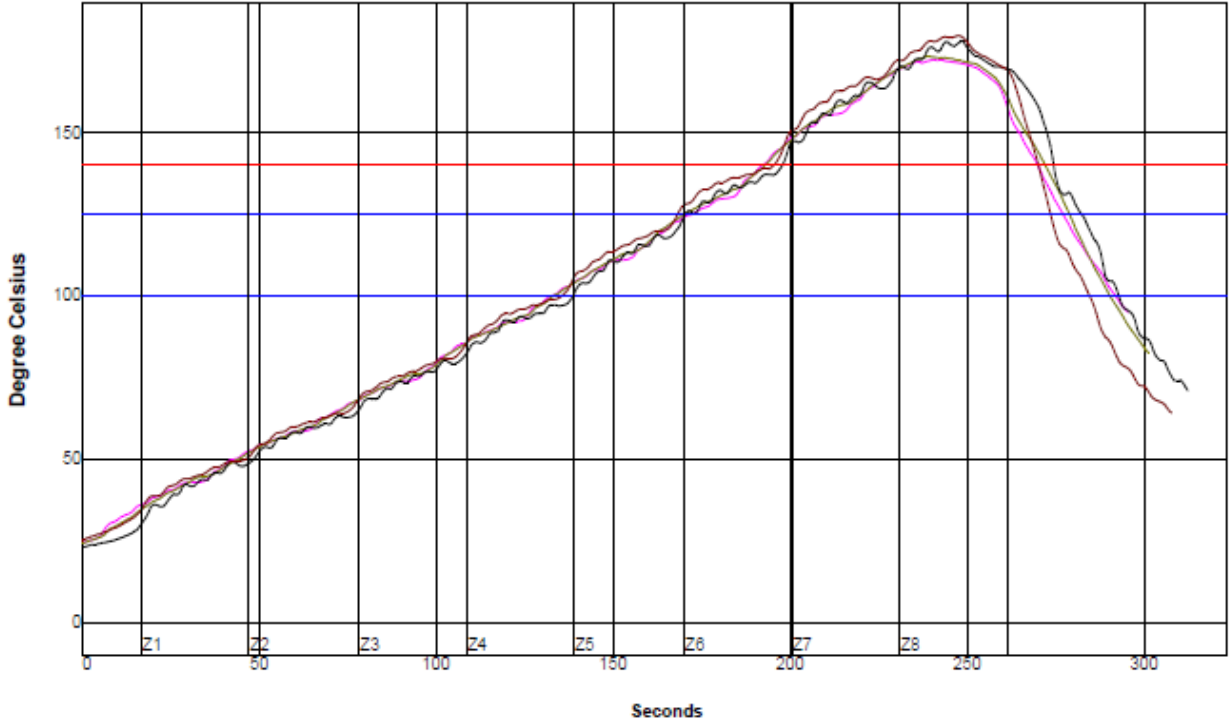
All solder pastes used were brought to room temperature prior to stencil printing. Common, commercially available equipment was used for test board preparation. Stencil printing used a 120 µm laser cut and electro-polished stencil with a nano-coating. The test board design (Figure 2) included print-to-fail patterns with challenging area ratios as well as areas for component placement. ENIG finish test boards were used for set-up, while reflow studies were carried out with fresh OSP copper boards.

The test matrix in Figure 1 shows which reflow profiles were tested for each alloy. These solder pastes were exposed to two different reflow profiles on virgin copper-OSP metalized boards. The reflow profiles varied in time-above-liquidus (time and temperature), peak oven temperature, and the conveyor speed (25 inches per minute and 11.3 inches per minute). Detailed profiles are provided in Figures 3 and 4.

Testing Matrix			
Conveyor Speed		25inches/min	11.3inches/min
Peak Oven Setting		190°C	205°C
TAL		TAL 140°C 165 Seconds	TAL 120°C 120 Seconds
Solder Paste	Baseline	x	x
	Bismuth 1	x	x
	Bismuth 2	x	x
	Indium		x

Figure 1: Testing Matrix

Setpoints (Degree Celsius)									
Zone	1	2	3	4	5	6	7	8	
Top	50	65	80	101	121	143	175	190	
Bottom	50	65	80	101	121	143	175	190	
Conveyor Speed (inch/min):		25.0							

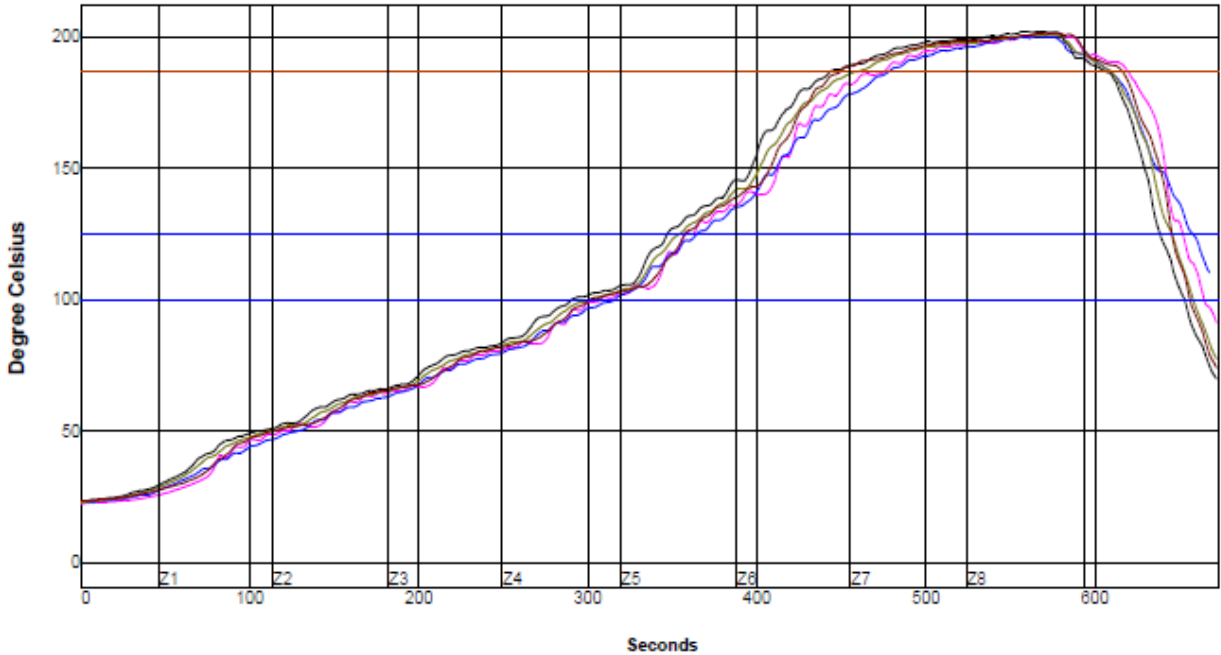


PW= 51%	Max Rising Slope	Soak Time 100-125°C		Reflow Time /140°C		Peak Temp		
<TC2>	1.05	5%	39.68	32%	77.77	-41%	172.27	-42%
<TC4>	0.97	-3%	36.85	23%	79.04	-37%	173.28	-34%
<TC5>	1.15	15%	31.71	6%	76.62	-45%	177.90	3%
<TC6>	1.20	20%	32.68	9%	74.74	-51%	179.71	18%
Delta	0.23		7.97		4.30		7.44	

Figure 3. Fast reflow profile with conveyor speed of 25 in/min

Setpoints (Degree Celsius)								
Zone	1	2	3	4	5	6	7	8
Top	50	65	79	102	140	194	201	205
Bottom	50	65	79	102	140	194	201	205

Conveyor Speed (inch/min): 11.3



PWI= 88%	Max Rising Slope	Max Falling Slope	Soak Time 100-125°C	Peak Temp	Tot Time #187°C					
<TC2>	1.35	35%	-2.67	16%	49.95	66%	201.54	54%	143.97	-40%
<TC3>	0.85	-15%	-1.60	70%	48.46	62%	200.51	40%	131.03	-72%
<TC4>	1.07	7%	-2.24	38%	53.06	77%	201.22	50%	149.65	-26%
<TC5>	1.16	16%	-2.47	27%	56.37	88%	202.40	65%	162.94	7%
<TC6>	1.22	22%	-2.77	11%	56.12	87%	201.78	57%	166.77	17%
Delta	0.50		1.17		7.91		1.89		35.74	

Figure 4. Slow reflow profile with conveyor speed of 11.3 in/min

PRINT QUALITY RESULTS

The printing procedure is designed to test solder pastes resilience to a pause mechanism. In this test, there was one, 1-hr pause presented after printing 12 PCBs, performing an under stencil wipe, and then progressing with printing an additional 12 PCBs. The test vehicle is pictured above in Figure 2. All of the volumetric data for the print quality section was analyzed using JMP® Statistical Software from SAS. That same data was then separated using the Variability/Attribute Gauge Chart function by the following characteristics:

- Alloy selection
- Aperture size
- Aperture shape
- Mask characteristics

In order to compare the five different lots across all of the different variables, a spreadsheet containing 21,901,152 cells of data was created. In order to separate the data efficiently, a naming convention was used for each pad combination. A string of characters was created with the first three letters being either PTF (print-to-fail) or CHP (chip); followed by the size of the aperture in microns; a C or an M which denotes whether the pad is either *copper or mask defined; and finally the shape of the pad (square or circle). * The boards are denoted as copper defined even if the board metallization is another metal. In this test, all of the boards that were not reflowed were ENIG. This decision was based on trying to avoid confusion and promote consistency within the naming convention.

The printing and solder paste variables, along with the board number and paste type, are displayed on the x-axis in the Variability Chart, while the volume percent is positioned on the y-axis. The complete data set (Appendix) is structured by each aperture size in the following order:

1. 220 micron copper/mask defined circles and squares
2. 230 micron copper/mask defined circles and squares
3. 240 micron copper/mask defined circles and squares
4. 260 micron copper/mask defined circles and squares
5. 280 micron copper/mask defined circles and squares
6. 300 micron copper/mask defined circles and squares
7. 0201 Chip Pads 320 by 230 micron copper defined
8. 0402 Chip Pads 900 by 700 micron copper defined

The following variability charts show all of the above aperture sizes with copper (metal) defined, circles, and the 0201 and 0402 pads. The data displayed in **Figures 5–10** show comparison results of the different alloyed solder pastes. It is important to note that the data was taken using a 120µm Nano-Coated stencil. The printing parameters were all kept constant. **Appendix A** exhibits the data in its entirety.

The printing performance across the alloys is consistent to what would be expected of the area ratios for this stencil thickness. It was interesting to view how the indium-containing alloy seemed to experience more variation across the various aperture sizes compared to the bismuth equivalent. This may indicate that the flux chosen was not an ideal match.

The two novel bismuth alloys printed similarly to the baseline 57Bi 42Sn 1Ag alloy. There was an expectation that the solder pastes response-to-pause performance would be concerning. However, considering the aperture size and area ratios, they printed relatively well, especially as the apertures grew in size.

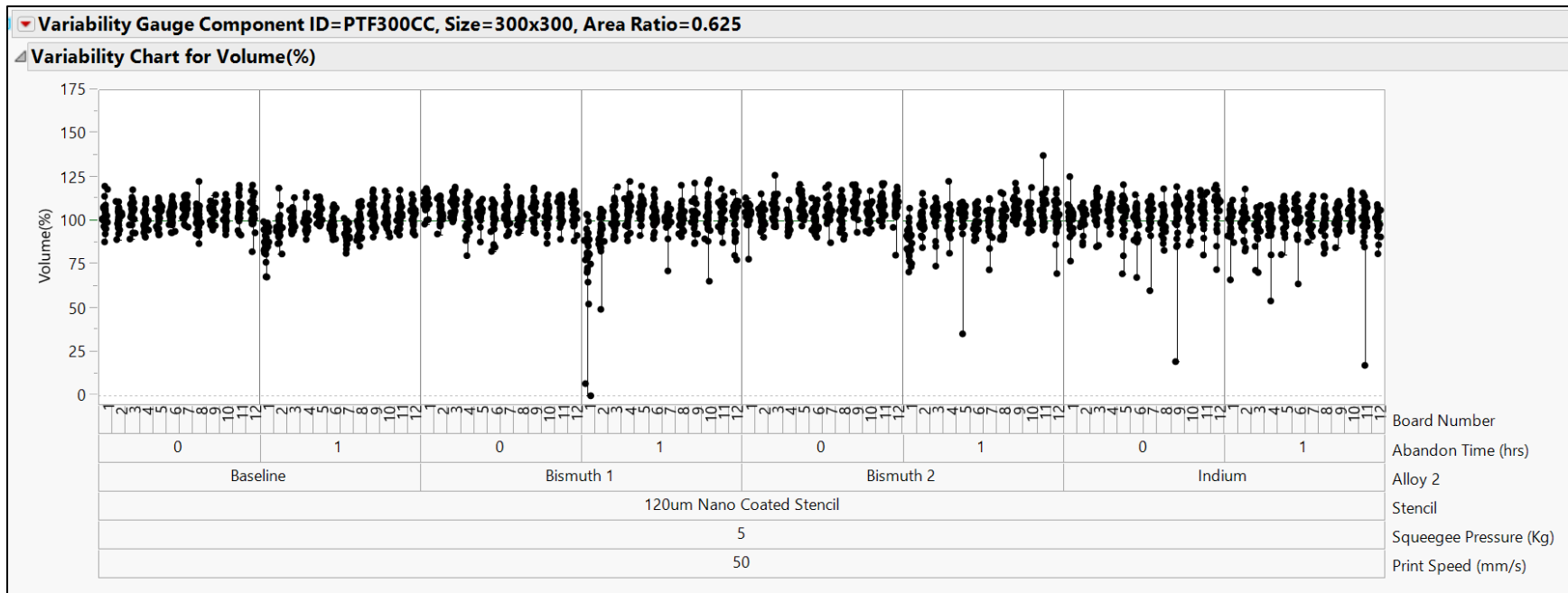


Figure 5. 300 μ m Copper Defined Circle Variability Chart

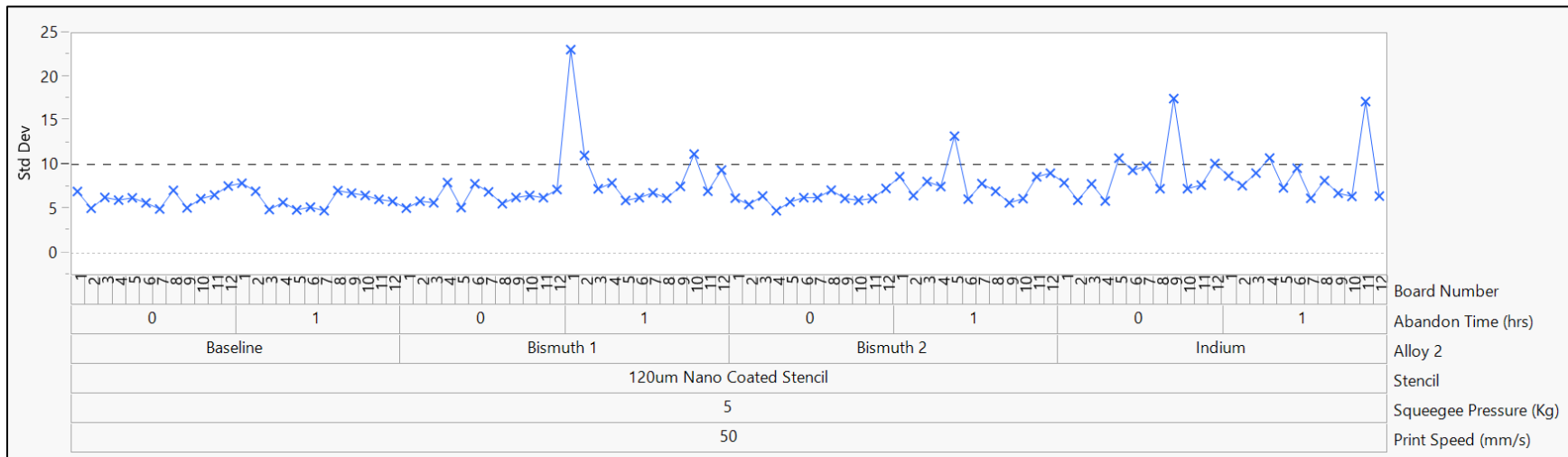


Figure 6. 300 μ m Copper Defined Circle Standard Deviation Chart

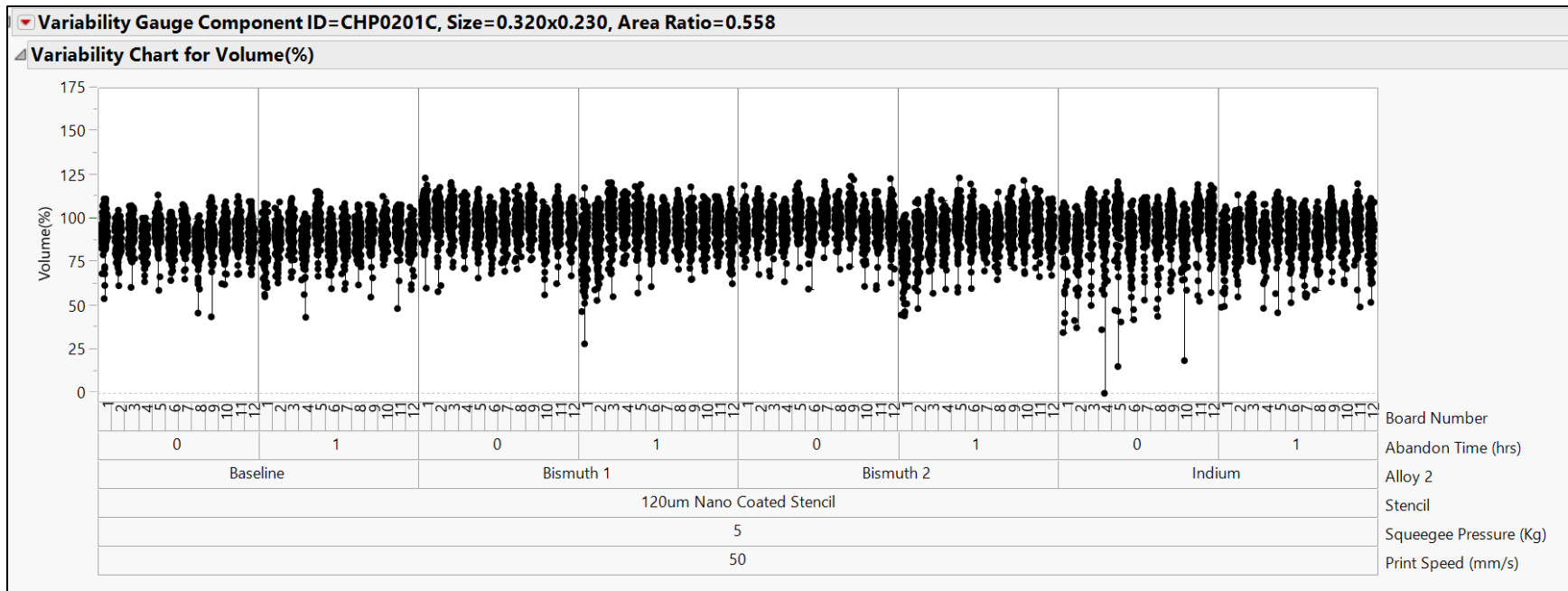


Figure 7. 0201 320x230 μ m Copper Defined Variability Chart

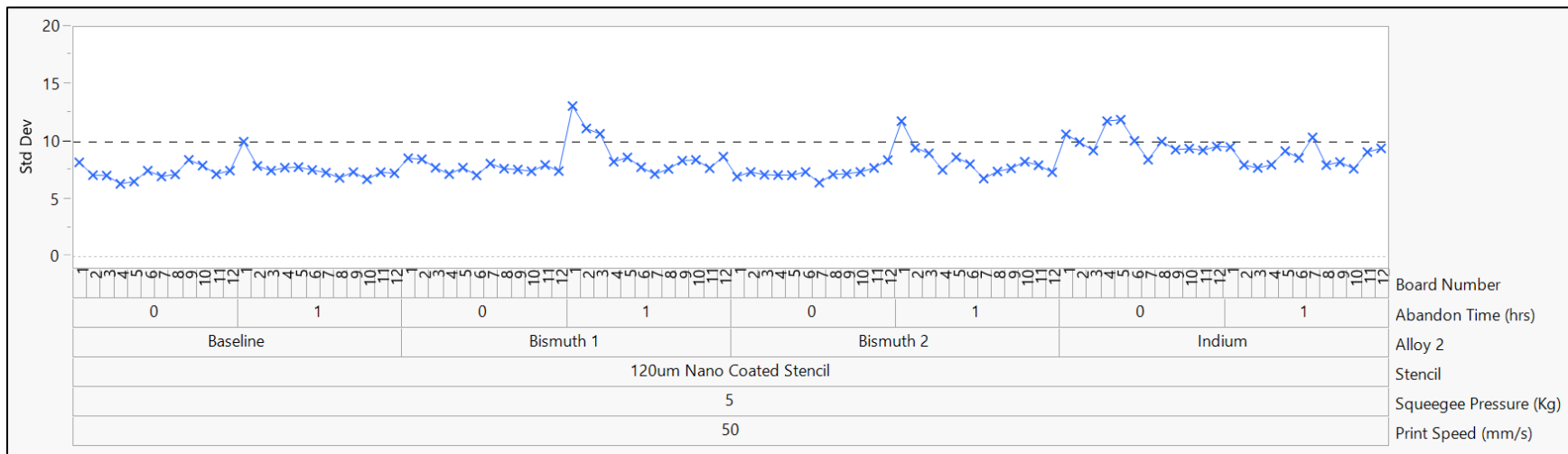


Figure 8. 0201 320x230 μ m Copper Defined Standard Deviation Chart

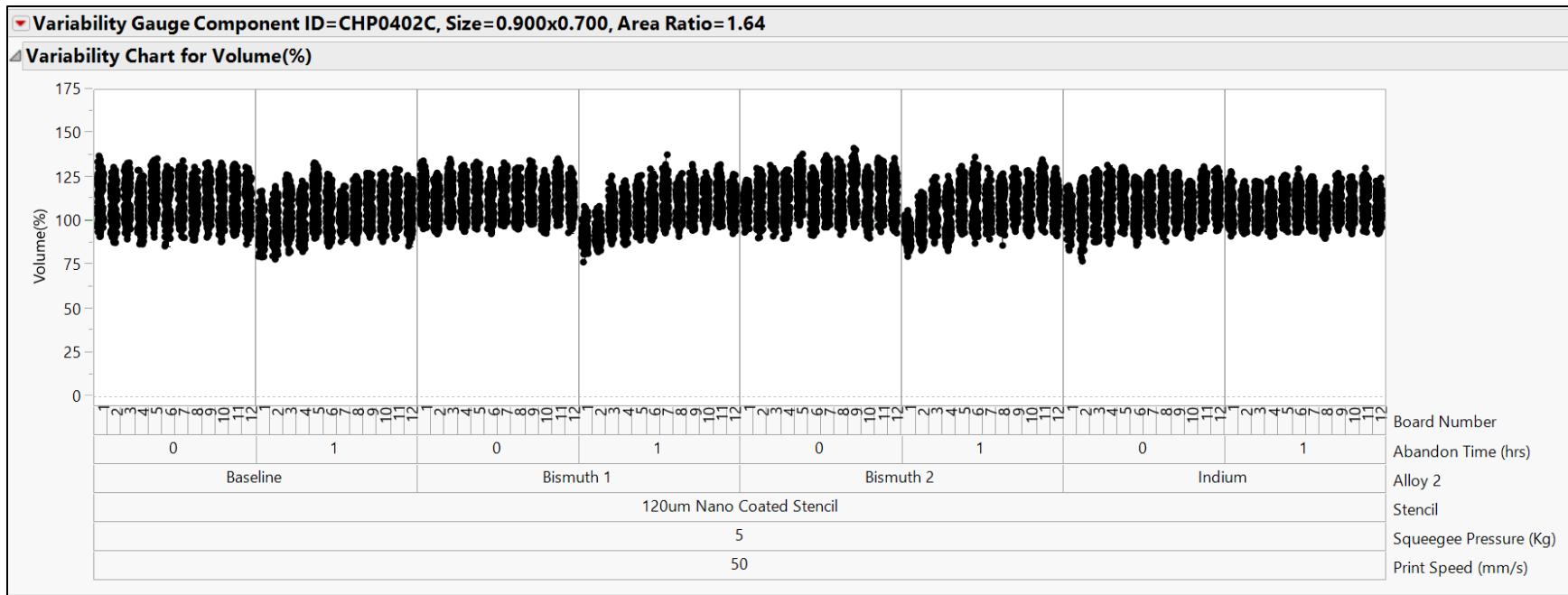


Figure 9. 0402 900x700 μ m Copper Defined Variability Chart

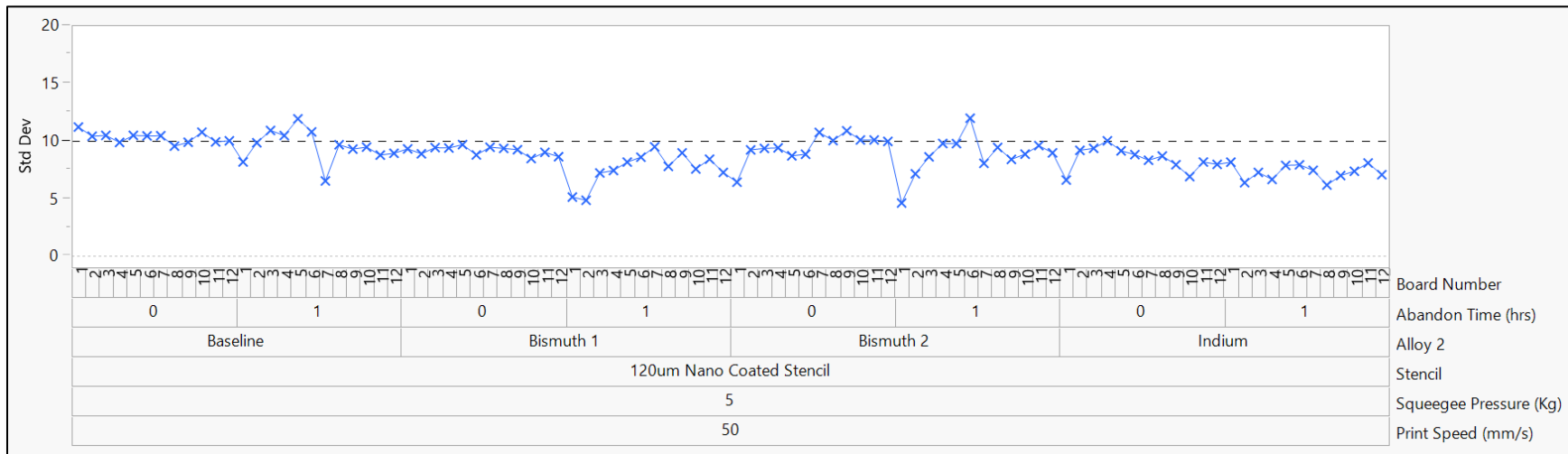


Figure 10. 0402 900x700 μ m Copper Defined Standard Deviation

REFLOW RESULTS

There were two different reflow profiles used in an eight-zone reflow oven. The “Slow” reflow process had a 205°C peak temperature, a conveyor speed of 11.3 inch/min, and a TAL (120°C) of 120 seconds (Figure 4). The “Fast” one had a 190°C peak temperature, but the conveyor speed was much faster (25 inch/min) with a TAL (140°C) of 165 seconds (Figure 3).

All three of the bismuth alloys were reflowed in both processes, and the indium-based one was only reflowed with the “Slow” reflow profile due to the peak temperature of the fast profile not being hot enough to promote adequate reflow. Examples of cross print and 0201 placement can be seen in Figures 11- 17.



Figure 11. Baseline Alloy with Slow Profile (L) Fast Profile (R)

In Figure 11, the difference is apparent in the number of pads that wet together; the slow profile exhibits more instances where the solder deposits coalesce on the cross print section of the test board. The Fast profile is a standard recommended profile for the bismuth-tin eutectic alloy and exhibits shinier solder deposits than the slower profile.



Figure 12. Bismuth Alloy 1 with Slow Profile (L) Fast Profile (R)

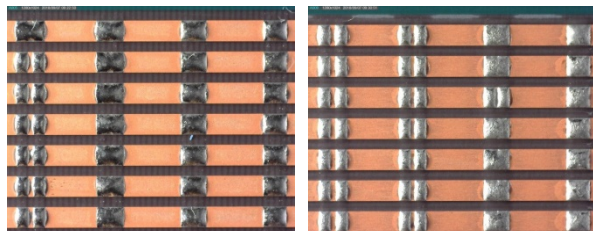


Figure 13. Bismuth Alloy 2 with Slow Profile (L) Fast Profile (R)

Figures 12 and 13 show that the fast profile offers better reflowed solder appearance and less bridging than using the slow profile.

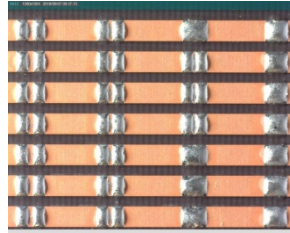


Figure 14. Indium Alloy with Slow Profile

The indium alloy (Figure 14) when compared to the bismuth alloys offers less bridging and shinier joints while looking at slow profile for comparison.

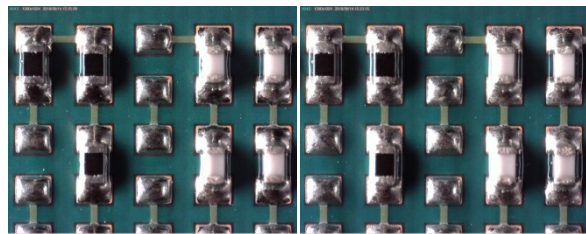


Figure 15. Baseline Alloy 0201 Placement Slow Profile (L) Fast Profile (R)

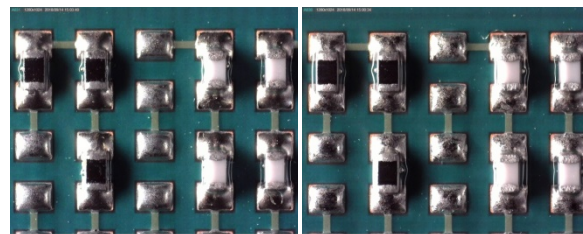


Figure 16. Bismuth Alloy 2 0201 Placement Slow Profile (L) Fast Profile (R)

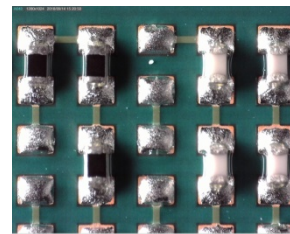


Figure 17. Indium Alloy 0201 Placement Slow Profile

Figures 15 and 16 show that the fast profile offers better reflowed solder appearance and less bridging than using the slow profile. The indium alloy (Figure 17), when compared to the bismuth alloys, offers less bridging and shinier joints while looking at slow profile for comparison.

The alloys in the placement portion of the test exhibited less difference and sensitivity to reflow profile than the cross printing portion. The preferred soldering profile for each alloy resulted in a more ideal solder joint appearance.

CONCLUSION

In conclusion, the differences between the alloys vary when considering which test you are investigating. The print quality test offers the conclusion that the bismuth alloys have better release, printability, and response-to-pause performance than the indium-containing one. While the reflow portion offers the opposite, the indium-containing alloy offers a more desirable appearing solder joint with the caveat that it was only reflowed using an optimized profile because the alloy would not reflow at the lower temperatures of the Fast profile which was adequate and ideal for the bismuth containing alloys. Since the same flux was used for all of the solder pastes in this study, there is no comparison to legacy solder pastes. But the printing performance on challenging area ratios clearly shows that the new materials are up to the standards expected for modern solder pastes. This will be critical to the development of low melting point solder pastes for the future.

FUTURE WORK

In the next phase of this research, BGA's and QFNs will be considered with regards to voiding performance. At this time further reliability tests will allow the opportunity to attempt to characterize how each of the alloys behaves in regards to long term reliability and failure modes.

ACKNOWLEDGMENTS

David Sbiroli – Technical Manager, Global Accounts, Indium Corporation
Eric Basow – Assistant Technical Manager, America's Region, Indium Corporation
Meagan Sloan – Technical Support Engineer, Indium Corporation
Rochester Institute of Technology

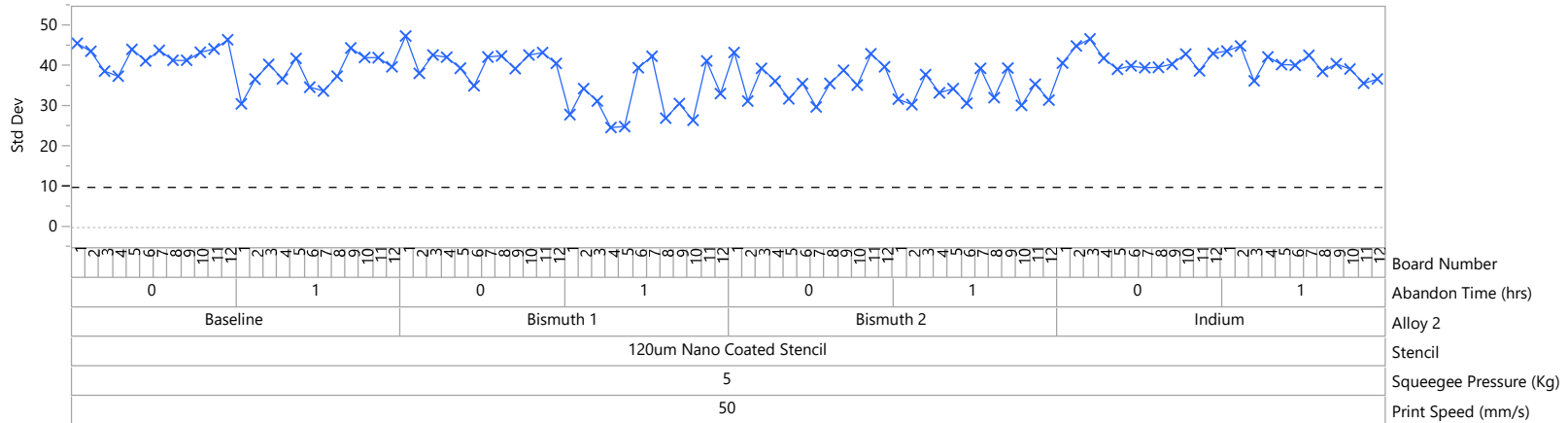
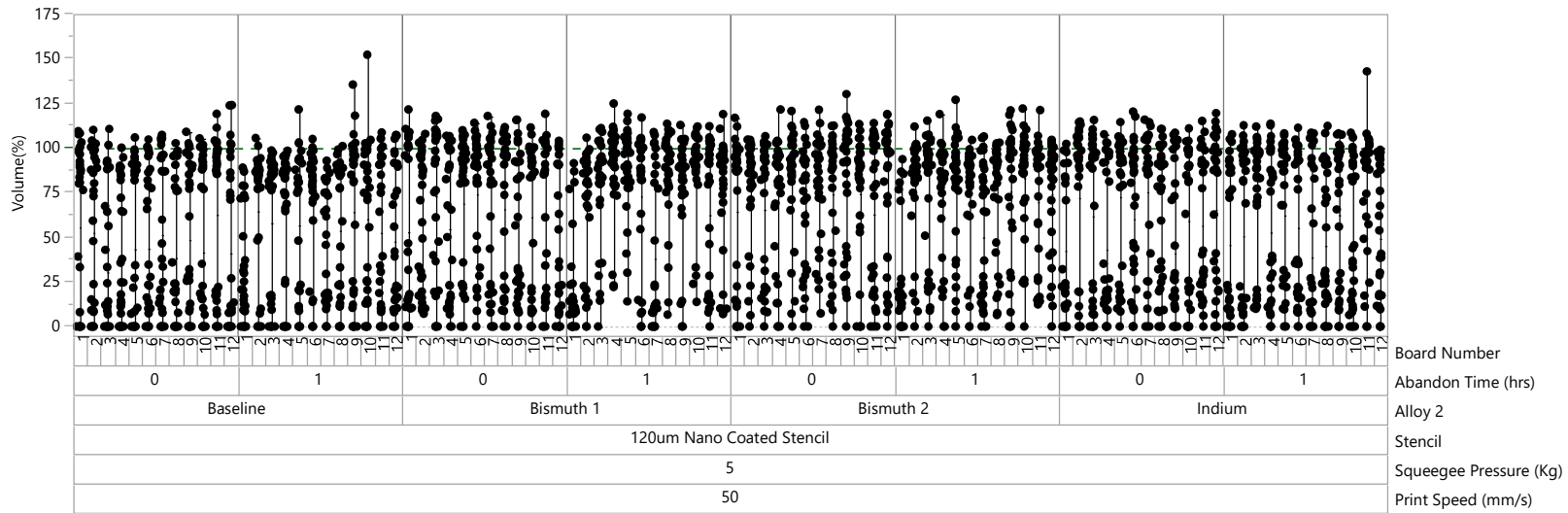
REFERENCES

- [1] 57Bi-42Sn-1Ag: A Lead Free, Low Temperature Solder for the Electronic Industry. Ernesto Ferrer and Helen Holder.
- [2] Aspandiar, R. et al. iNEMI Project on Process Development of BiSn-Based Low-Temperature Solder Pastes. SMTAi 2017.

Appendix A: Variability Chart

Variability Gauge Component ID=PTF220CC, Size=220x220, Area Ratio=0.458

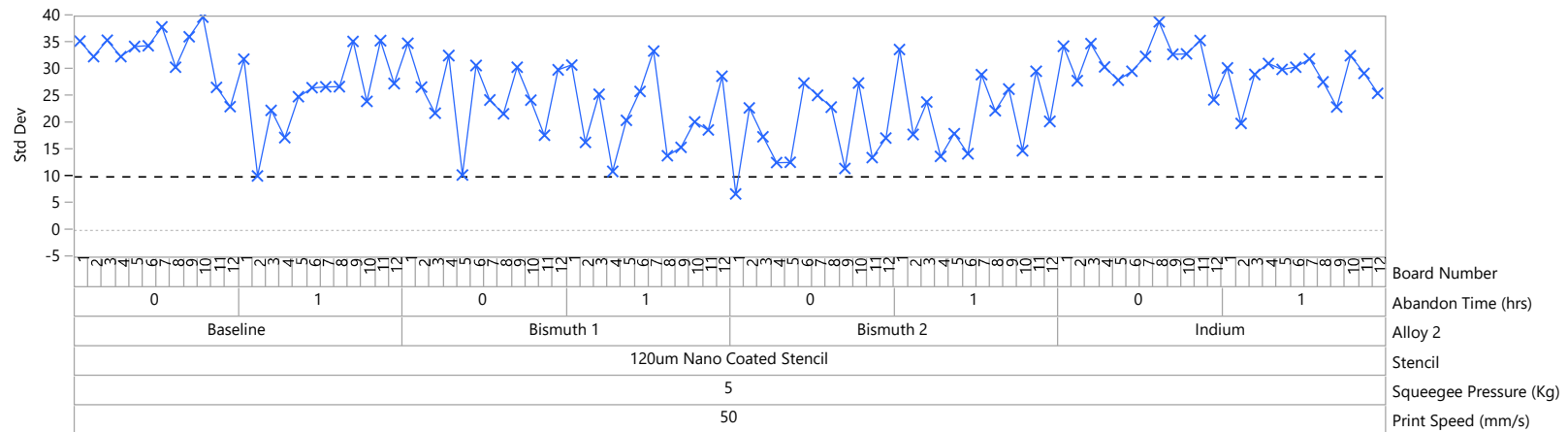
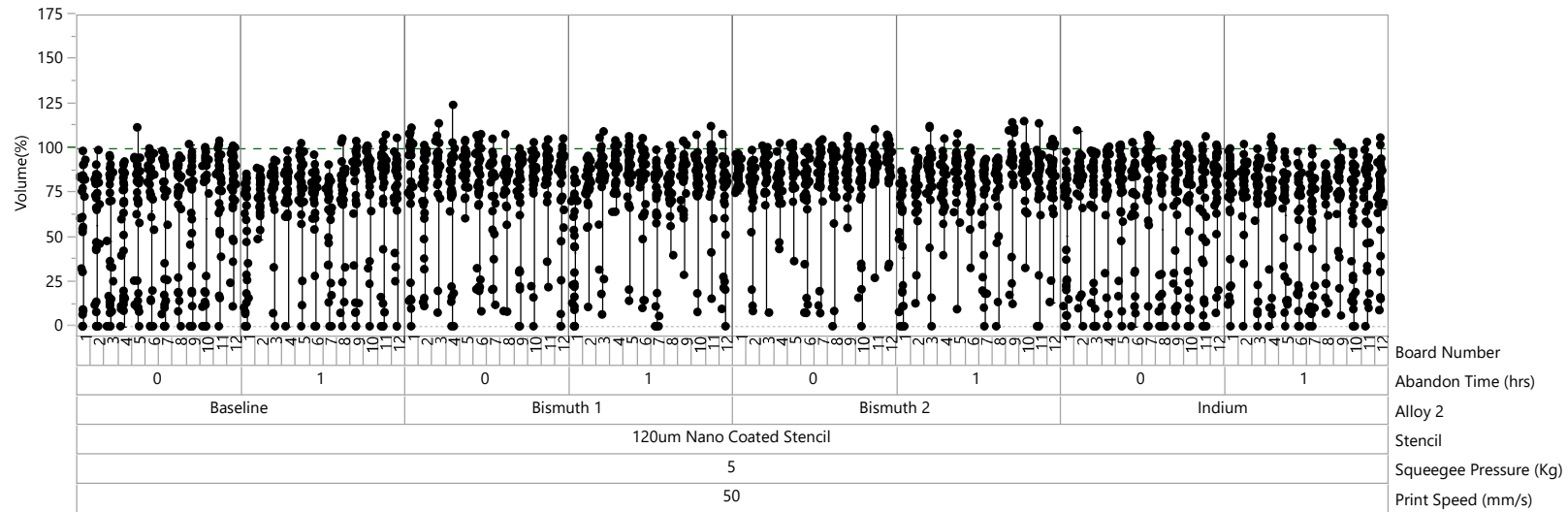
Variability Chart for Volume(%)



Report: Variability Chart

Variability Gauge Component ID=PTF220CS, Size=220x220, Area Ratio=0.458

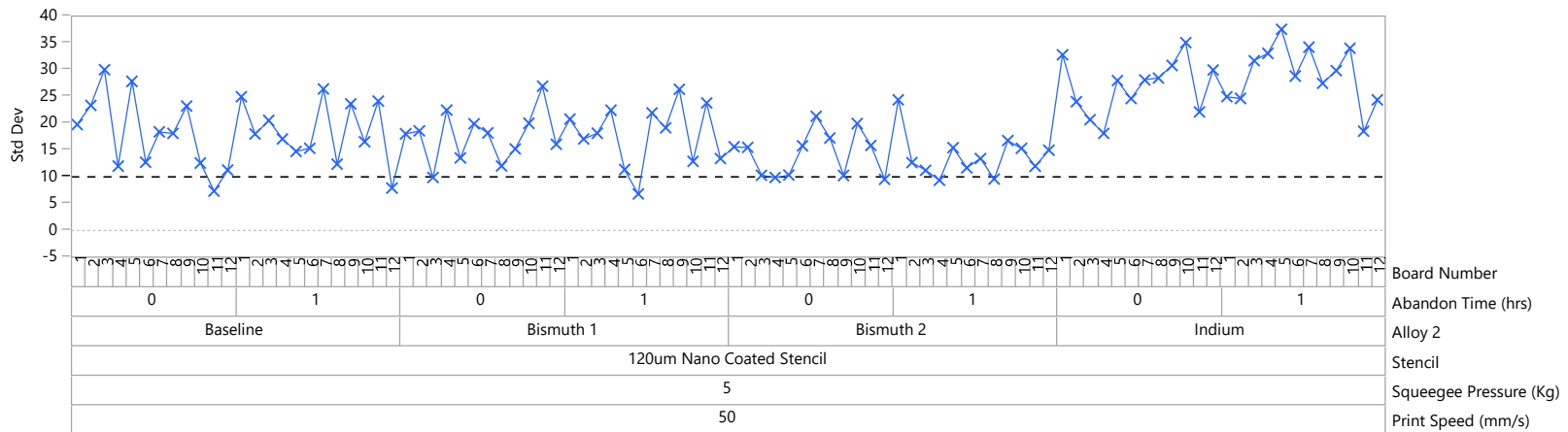
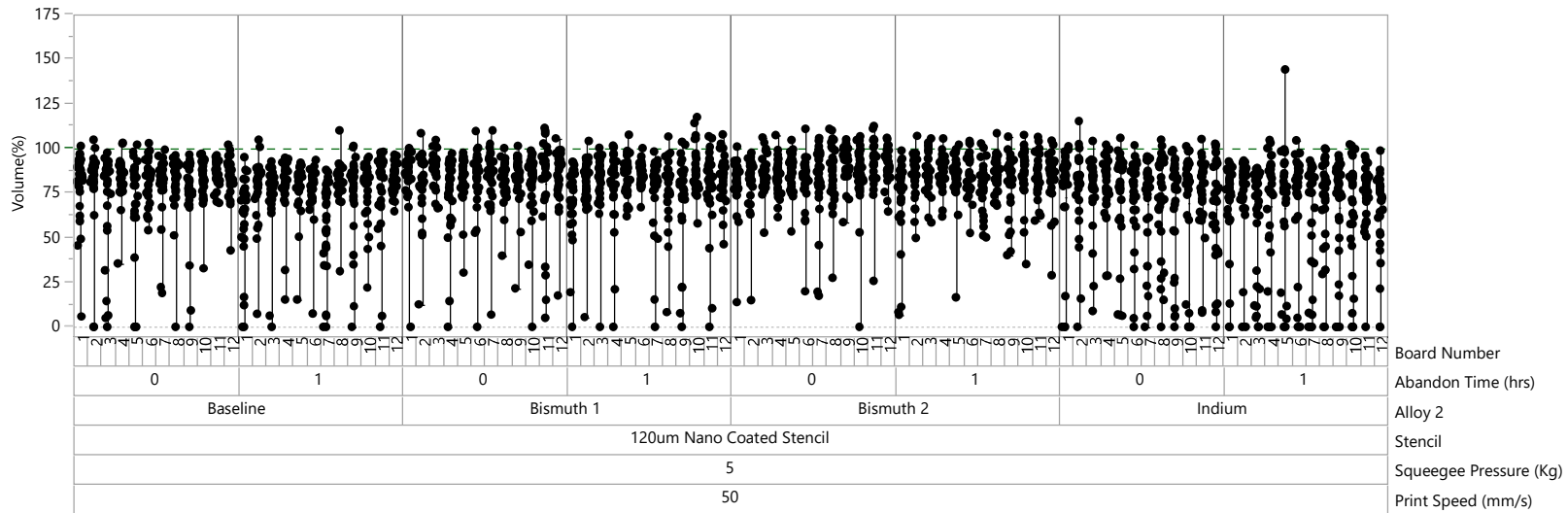
Variability Chart for Volume(%)



Report: Variability Chart

Variability Gauge Component ID=PTF220MC, Size=220x220, Area Ratio=0.458

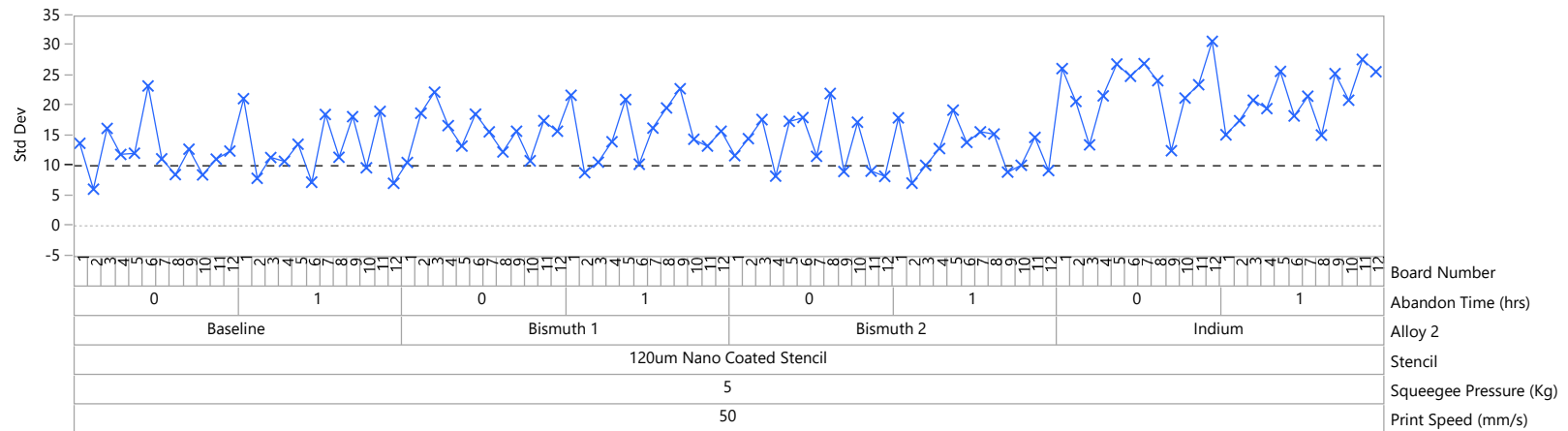
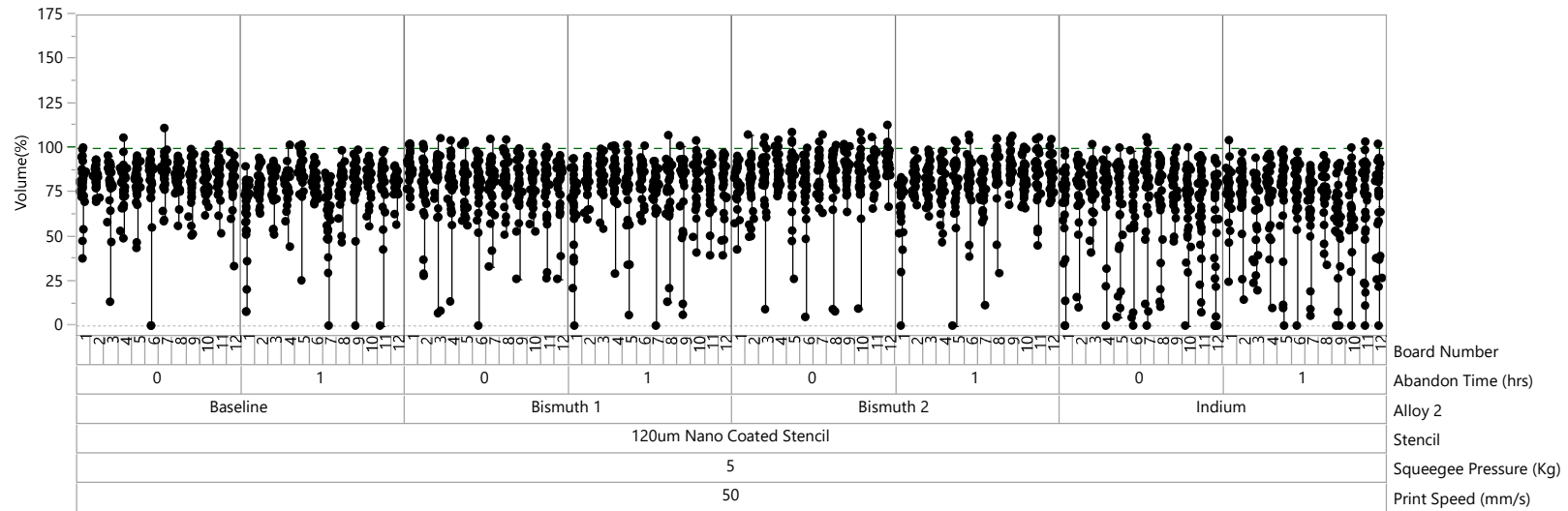
Variability Chart for Volume(%)



Report: Variability Chart

Variability Gauge Component ID=PTF220MS, Size=220x220, Area Ratio=0.458

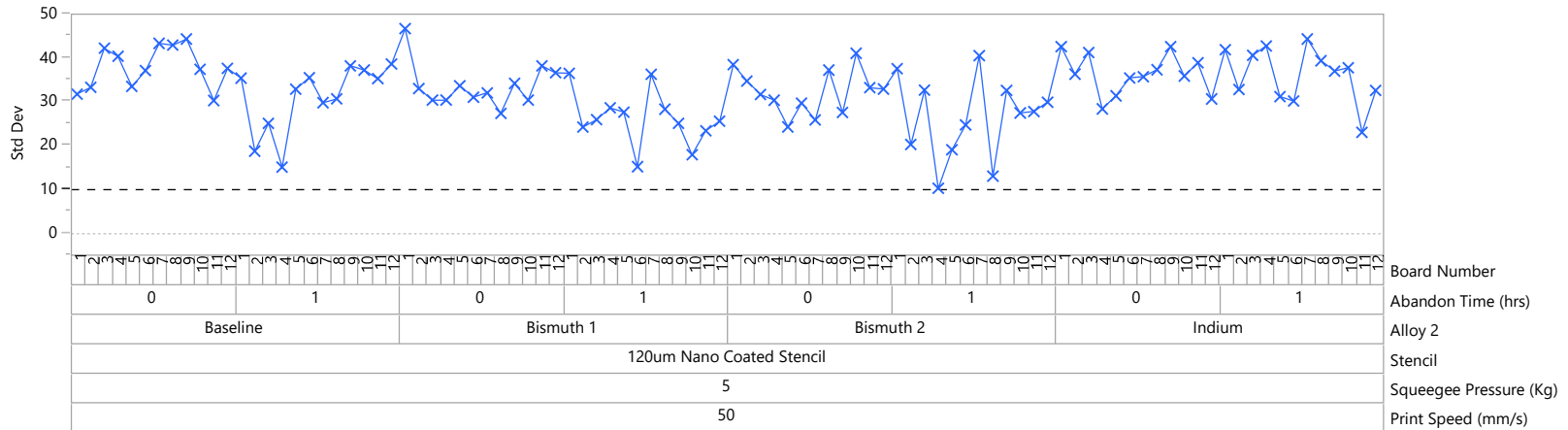
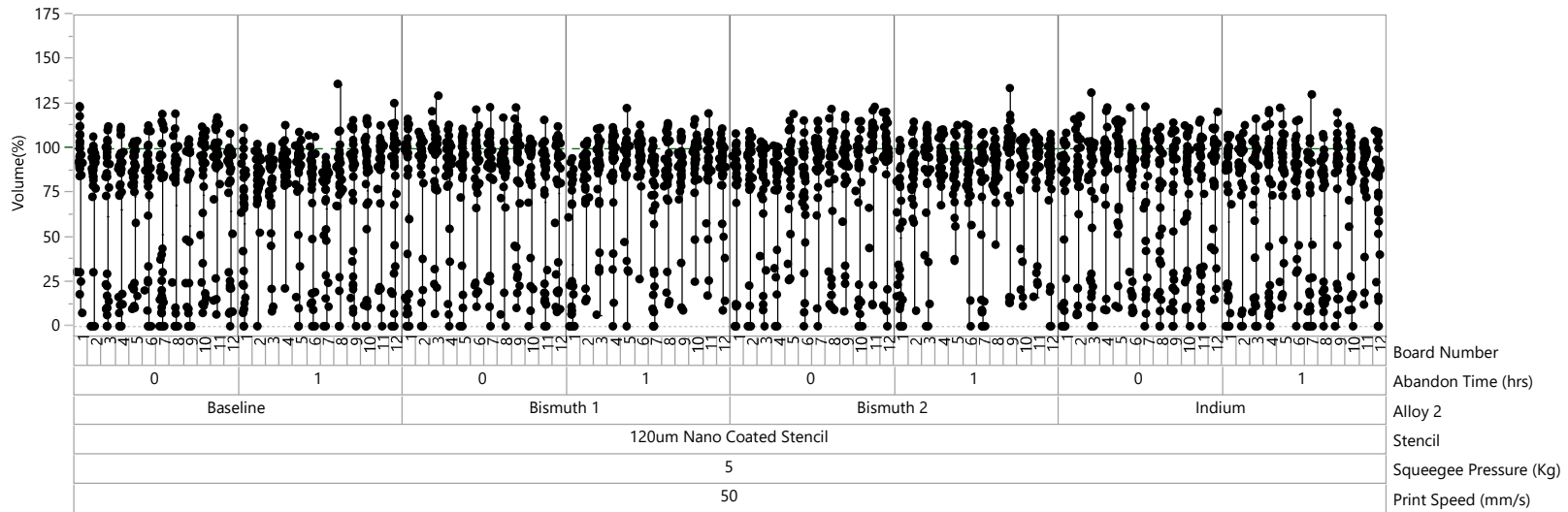
Variability Chart for Volume(%)



Report: Variability Chart

Variability Gauge Component ID=PTF230CC, Size=230x230, Area Ratio=0.479

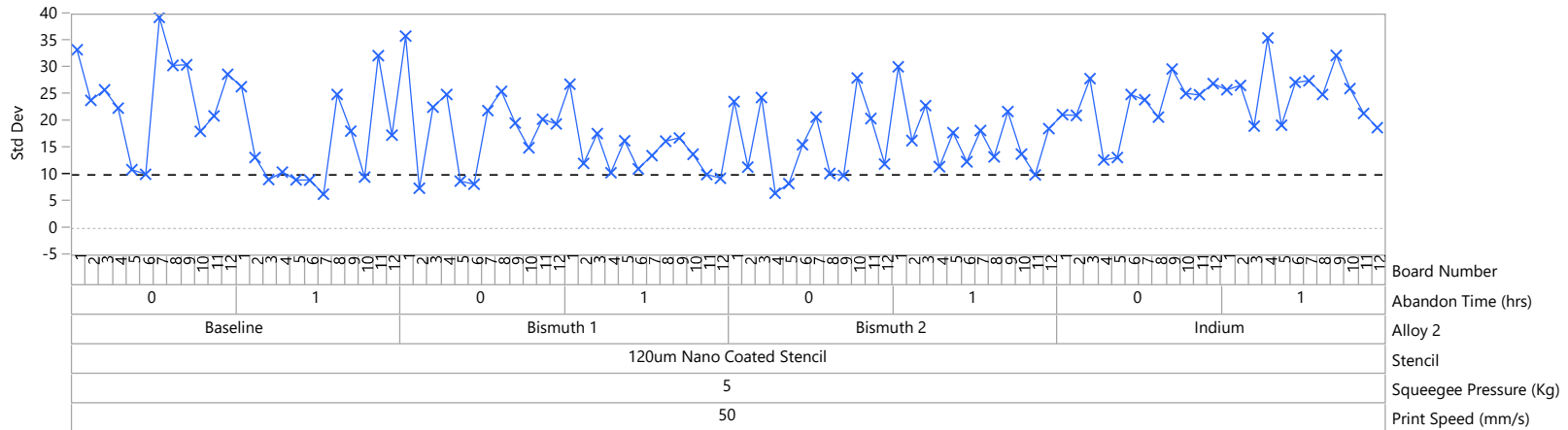
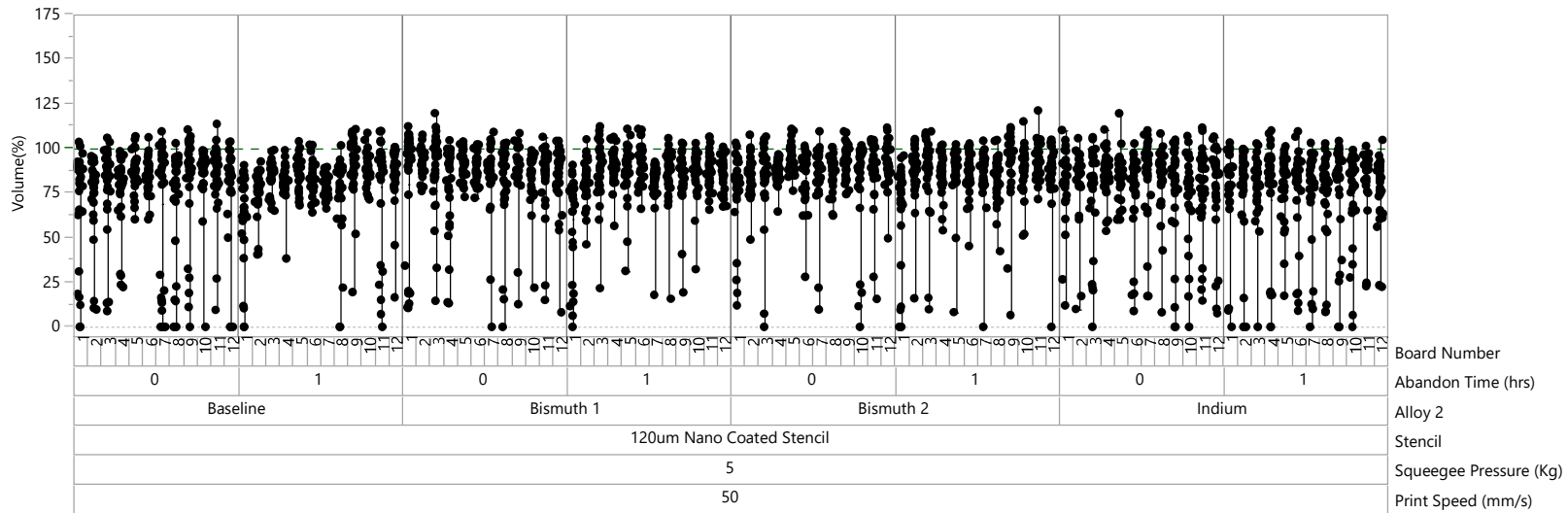
Variability Chart for Volume(%)



Report: Variability Chart

Variability Gauge Component ID=PTF230CS, Size=230x230, Area Ratio=0.479

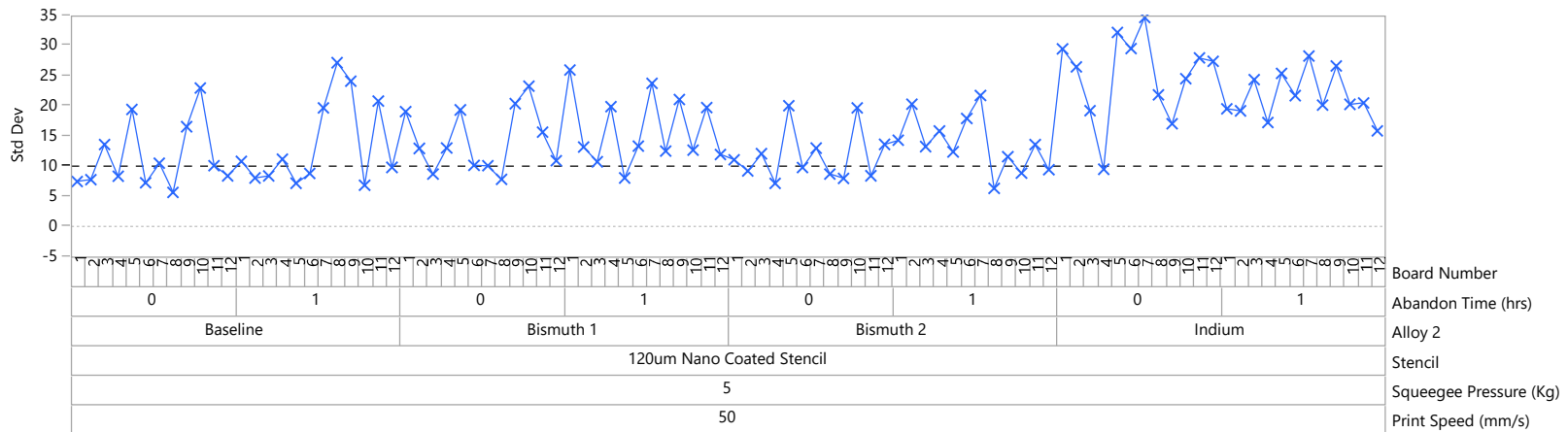
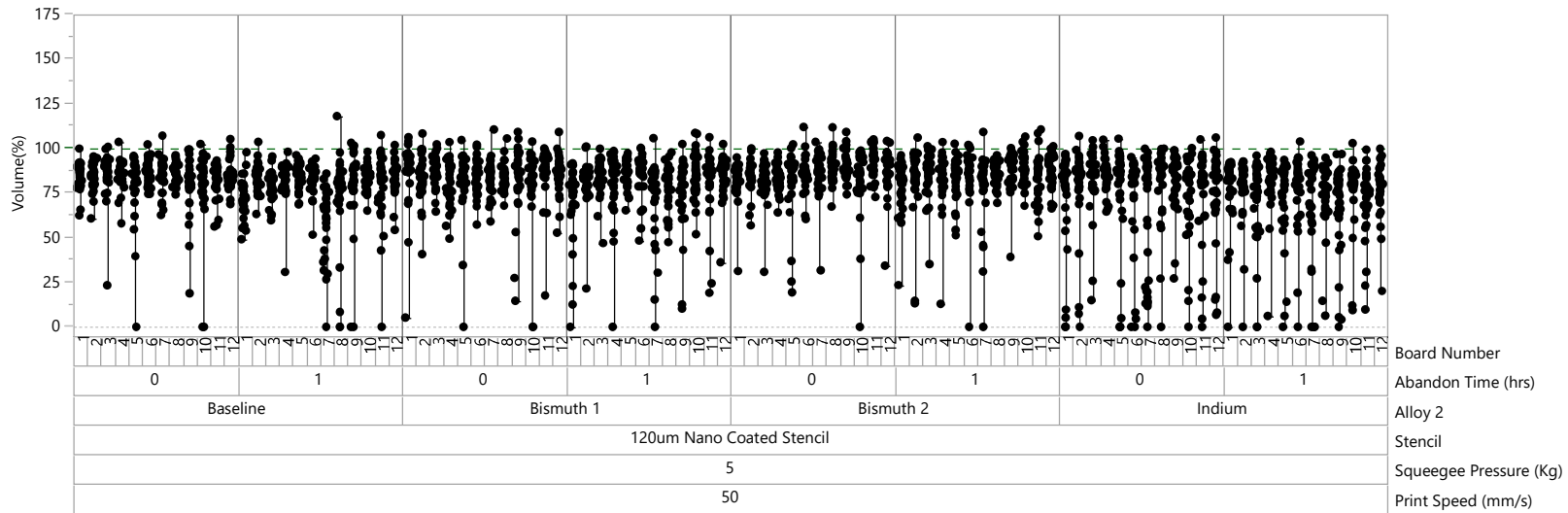
Variability Chart for Volume(%)



Report: Variability Chart

Variability Gauge Component ID=PTF230MC, Size=230x230, Area Ratio=0.479

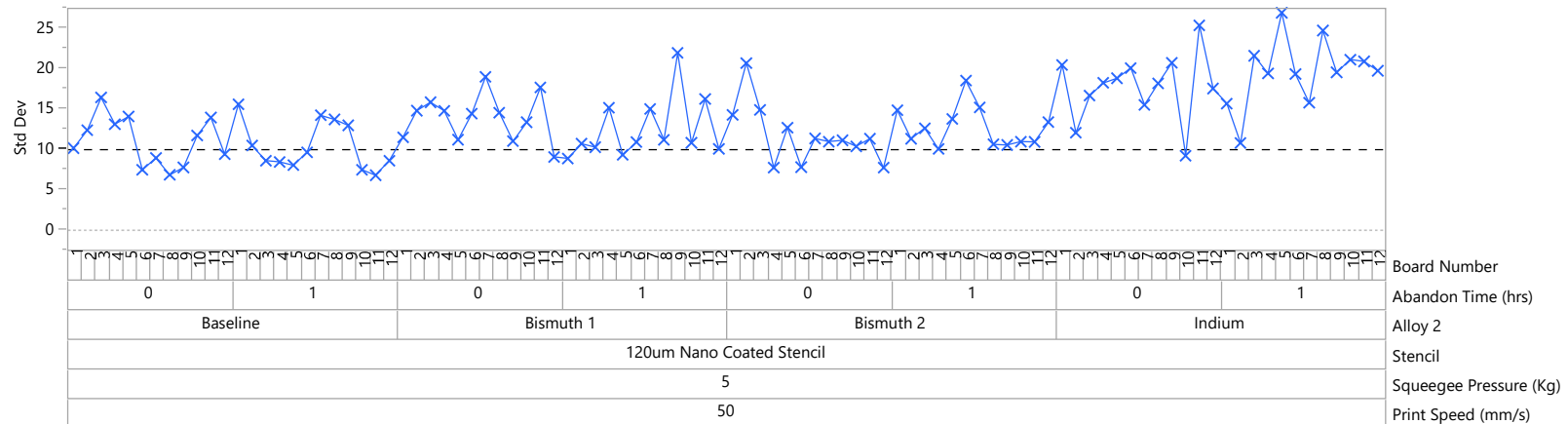
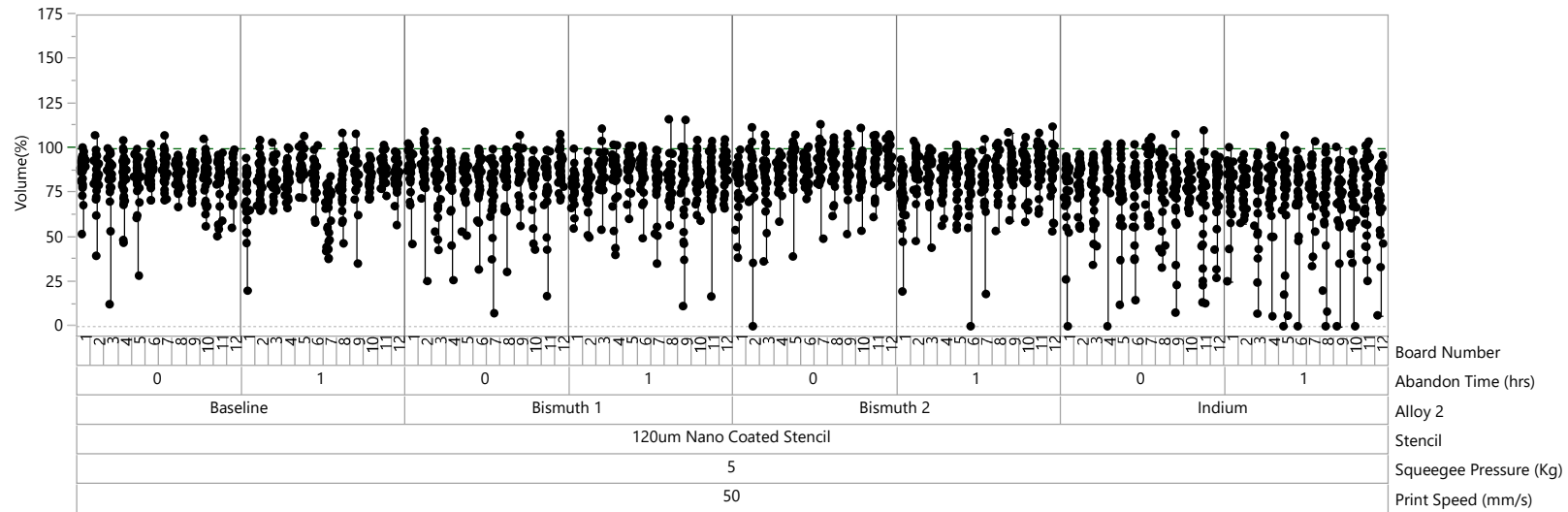
Variability Chart for Volume(%)



Report: Variability Chart

Variability Gauge Component ID=PTF230MS, Size=230x230, Area Ratio=0.479

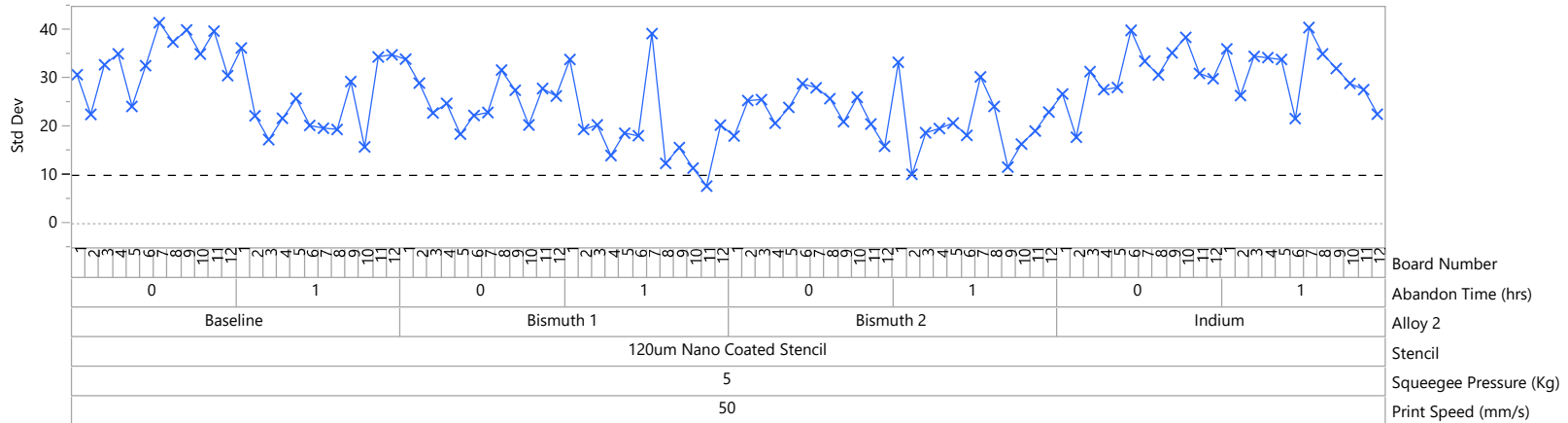
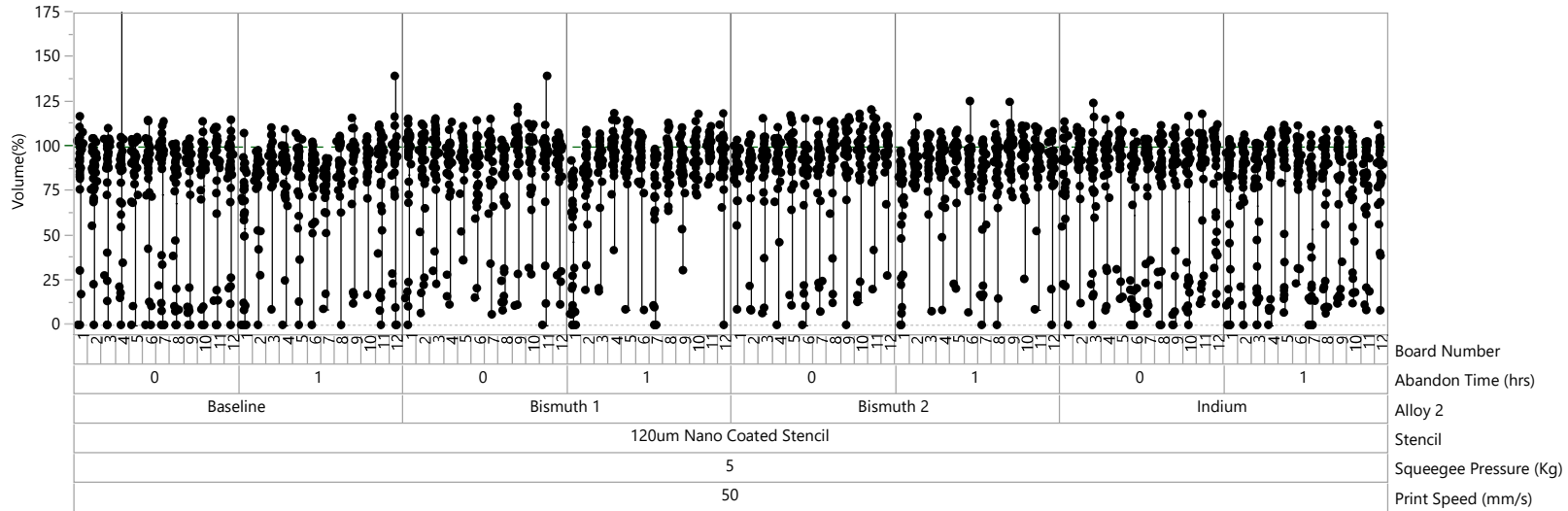
Variability Chart for Volume(%)



Report: Variability Chart

Variability Gauge Component ID=PTF240CC, Size=240x240, Area Ratio=0.5

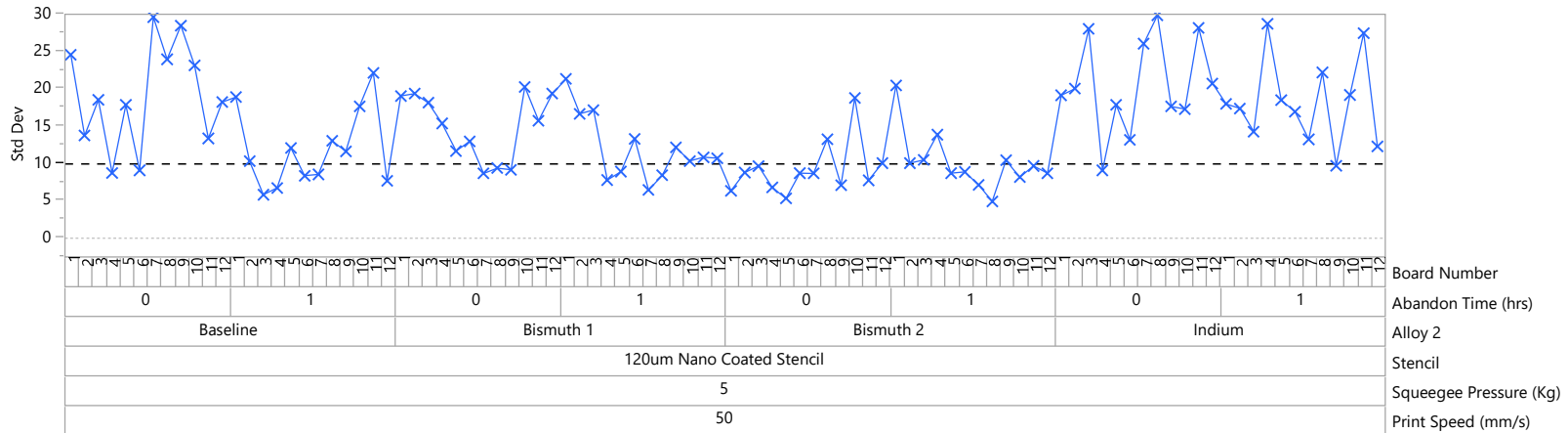
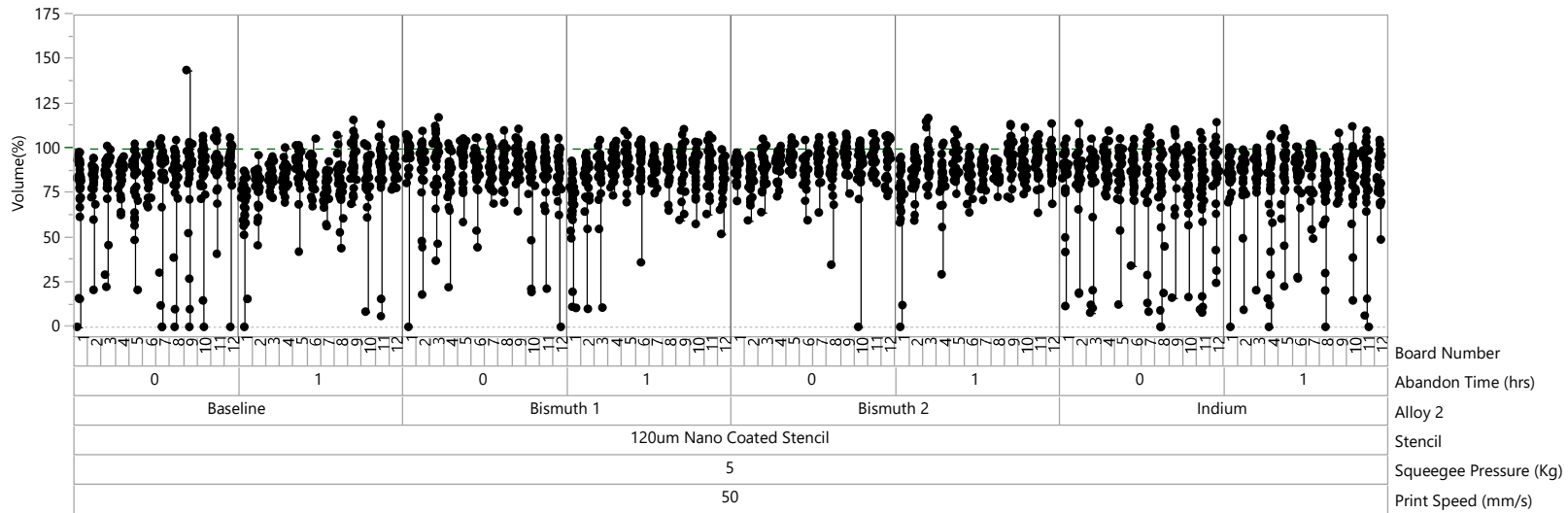
Variability Chart for Volume(%)



Report: Variability Chart

Variability Gauge Component ID=PTF240CS, Size=240x240, Area Ratio=0.5

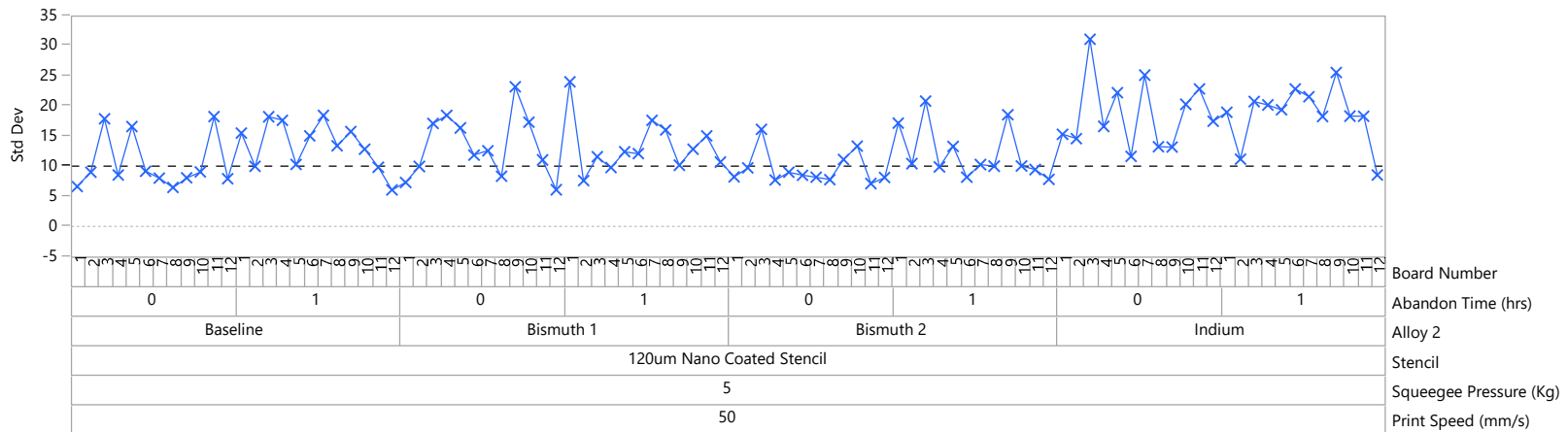
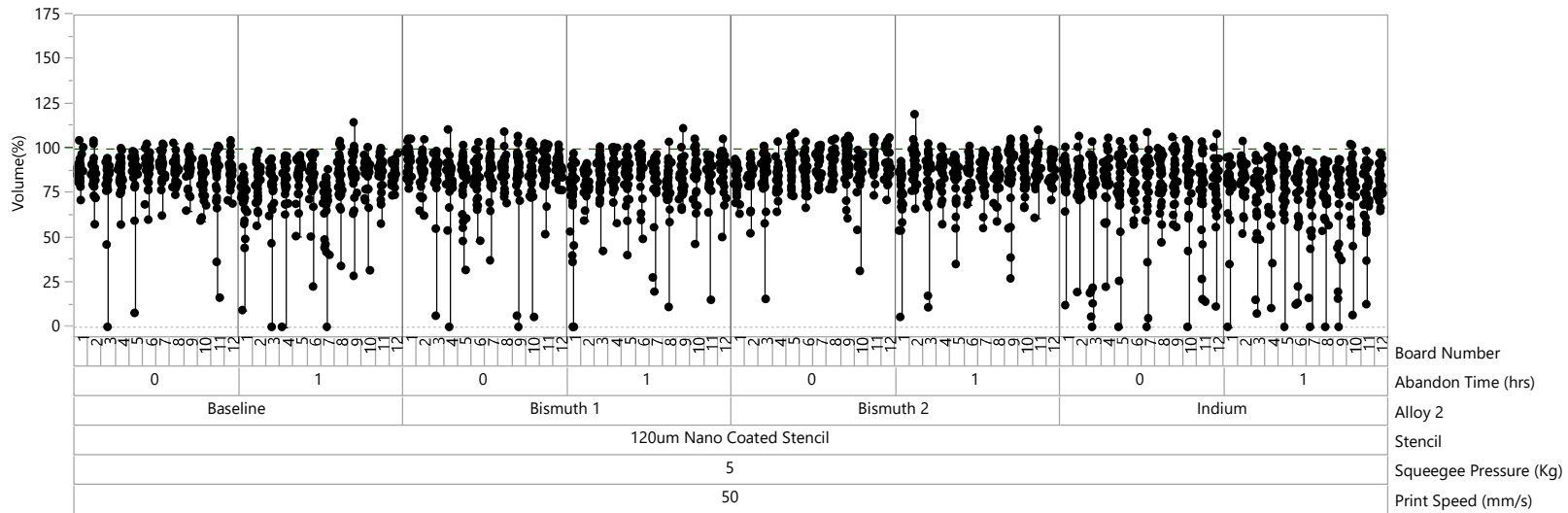
Variability Chart for Volume(%)



Report: Variability Chart

Variability Gauge Component ID=PTF240MC, Size=240x240, Area Ratio=0.5

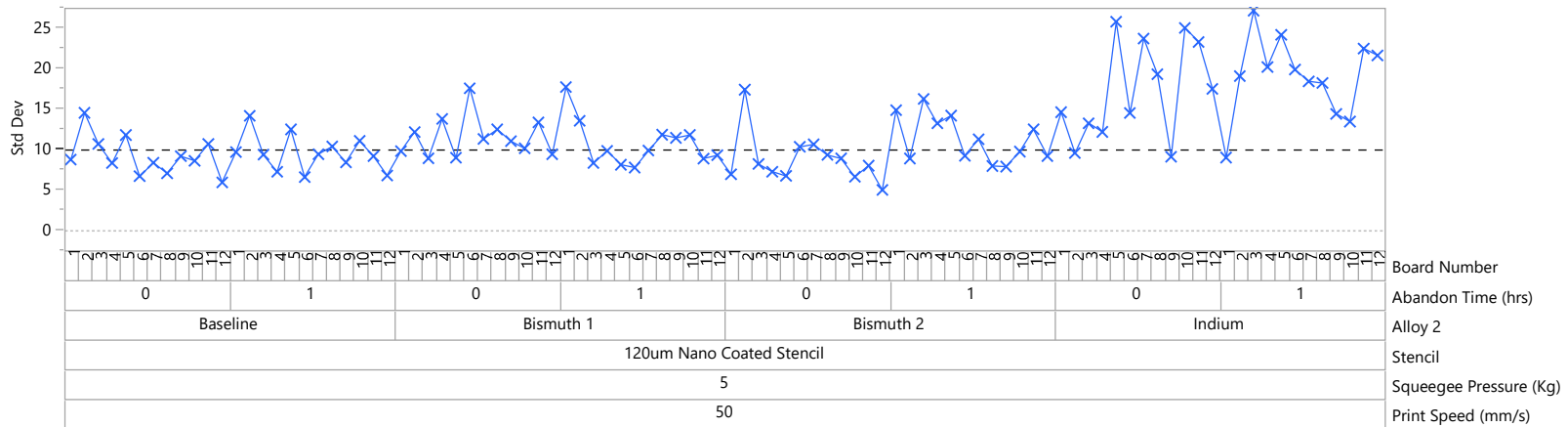
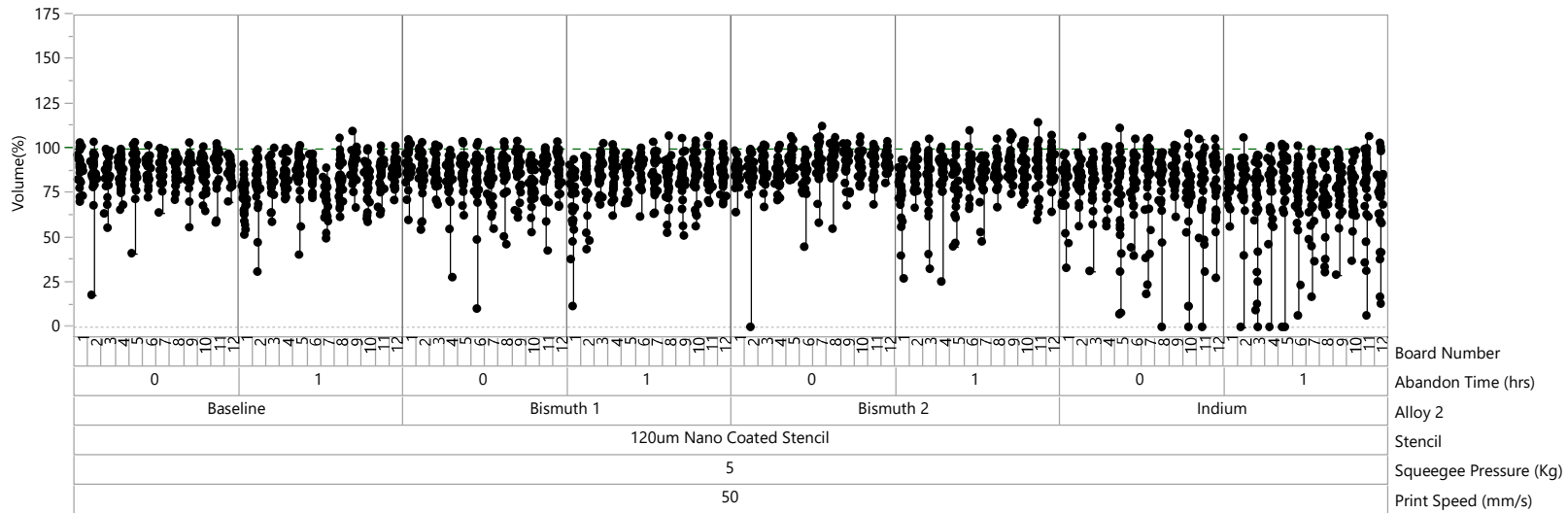
Variability Chart for Volume(%)



Report: Variability Chart

Variability Gauge Component ID=PTF240MS, Size=240x240, Area Ratio=0.5

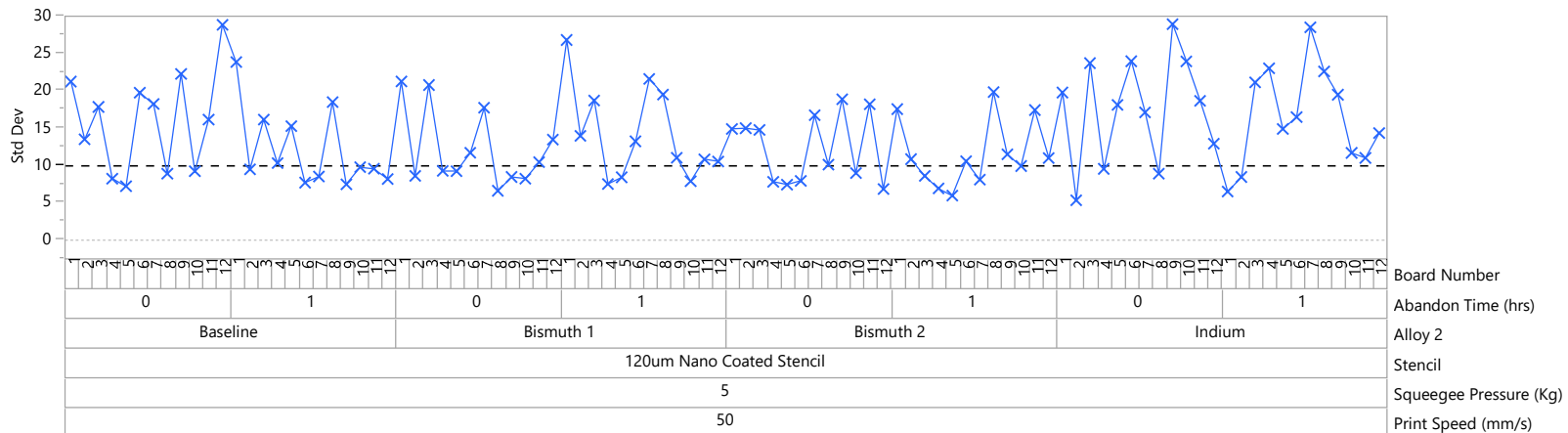
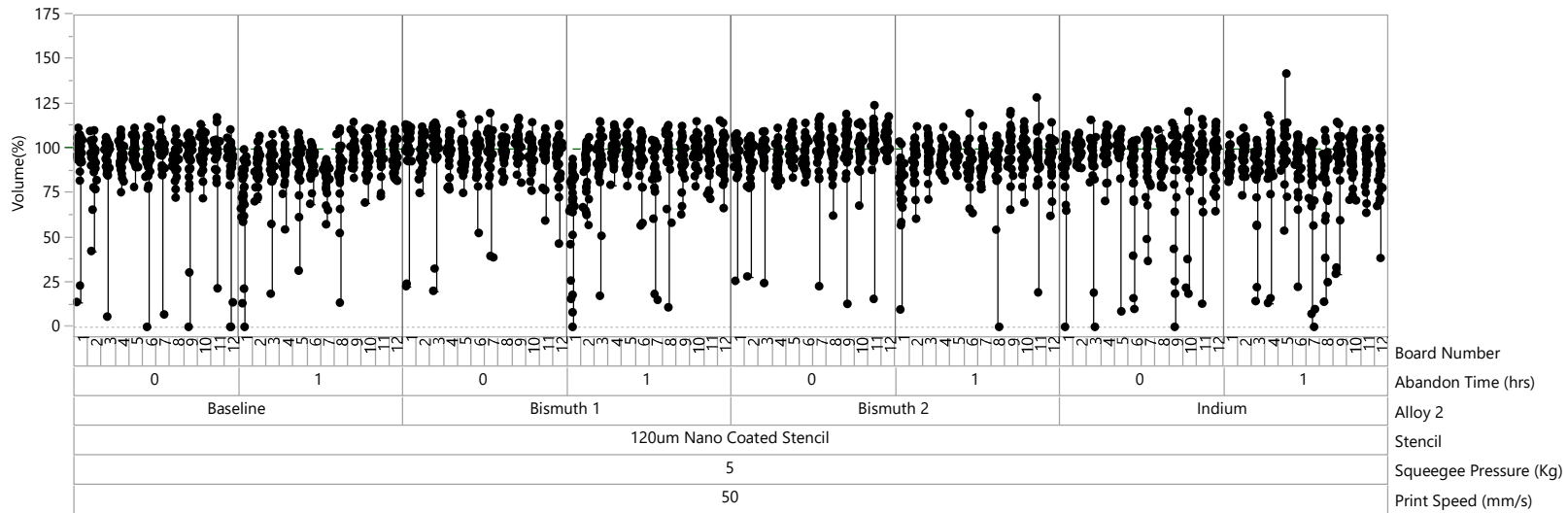
Variability Chart for Volume(%)



Report: Variability Chart

Variability Gauge Component ID=PTF260CC, Size=260x260, Area Ratio=0.542

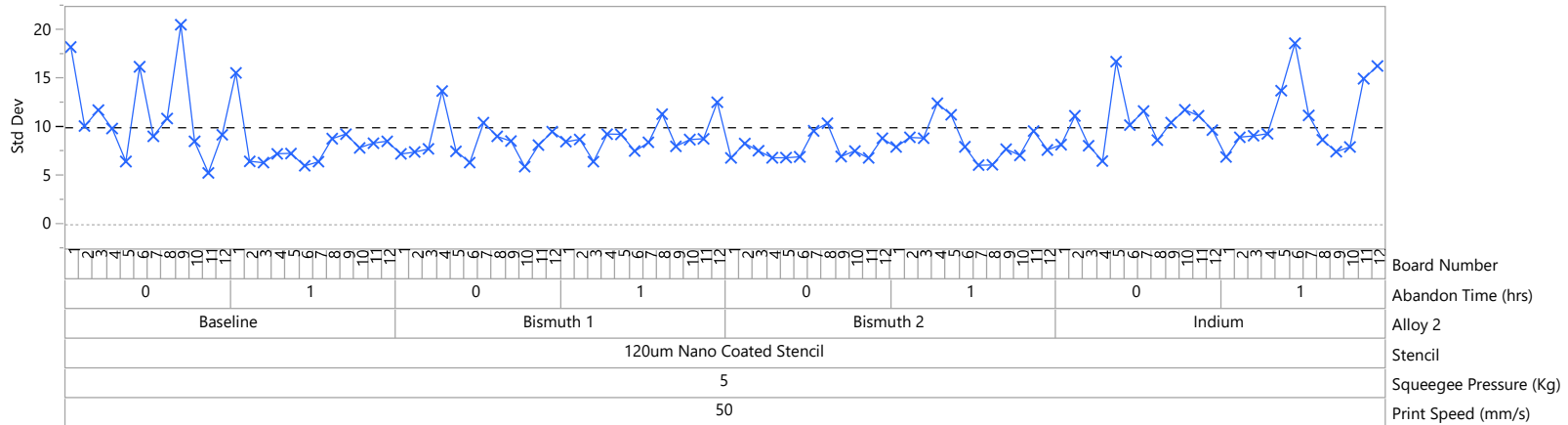
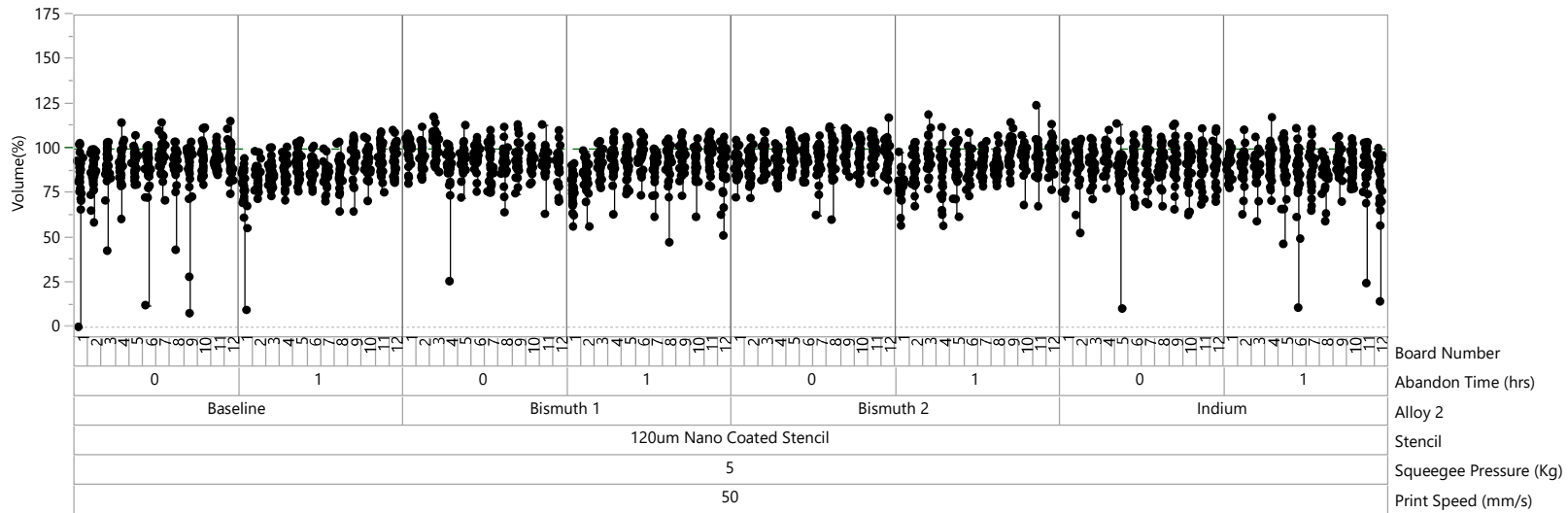
Variability Chart for Volume(%)



Report: Variability Chart

Variability Gauge Component ID=PTF260CS, Size=260x260, Area Ratio=0.542

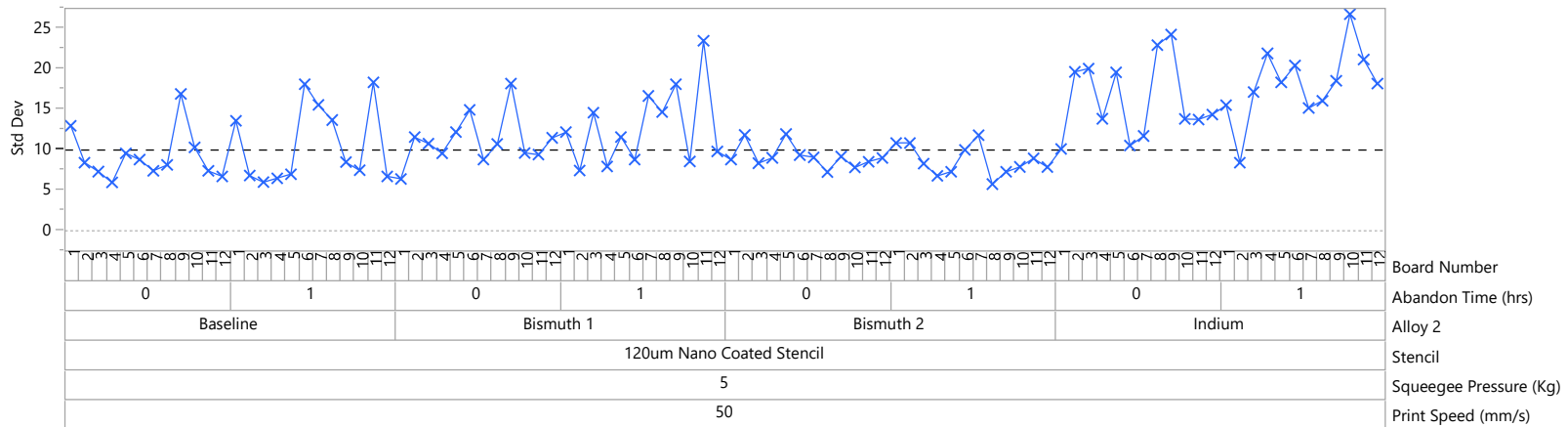
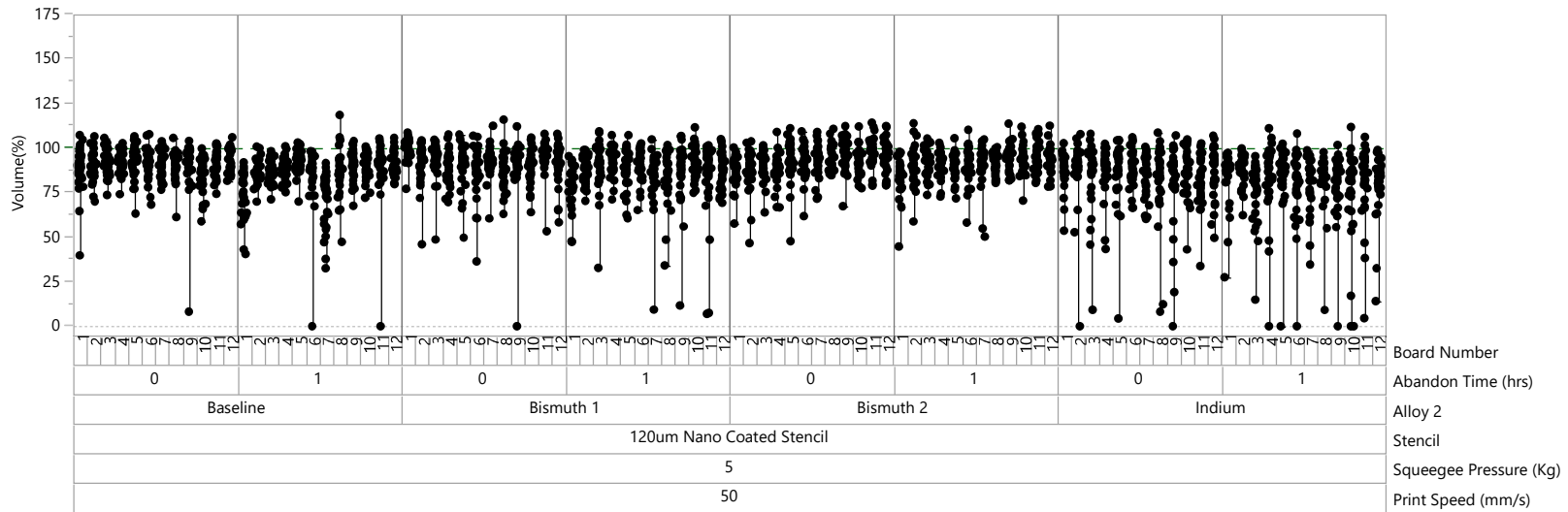
Variability Chart for Volume(%)



Report: Variability Chart

Variability Gauge Component ID=PTF260MC, Size=260x260, Area Ratio=0.542

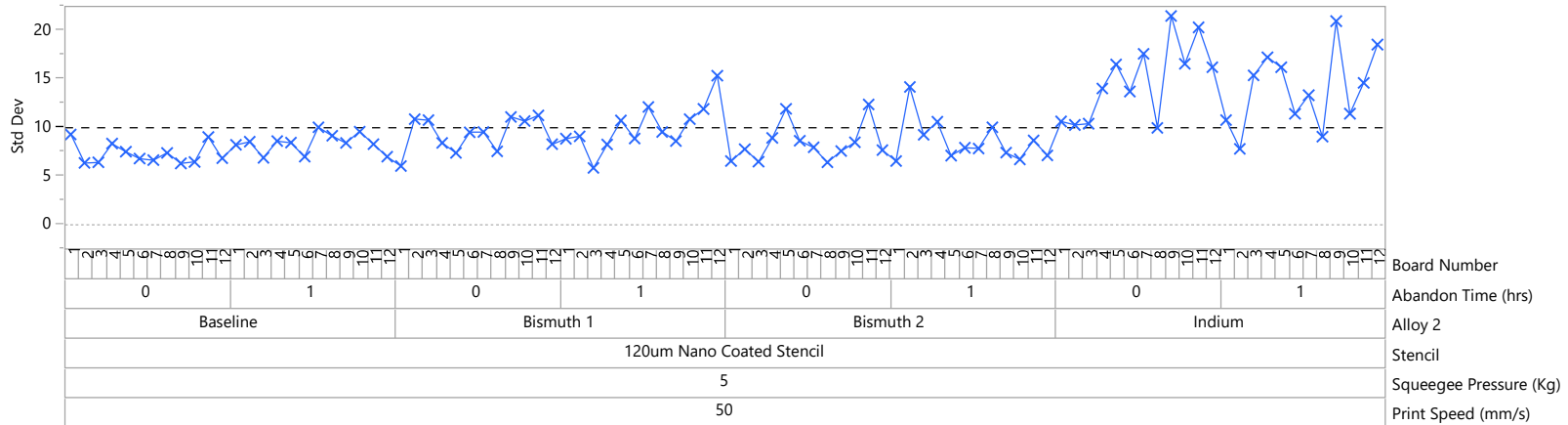
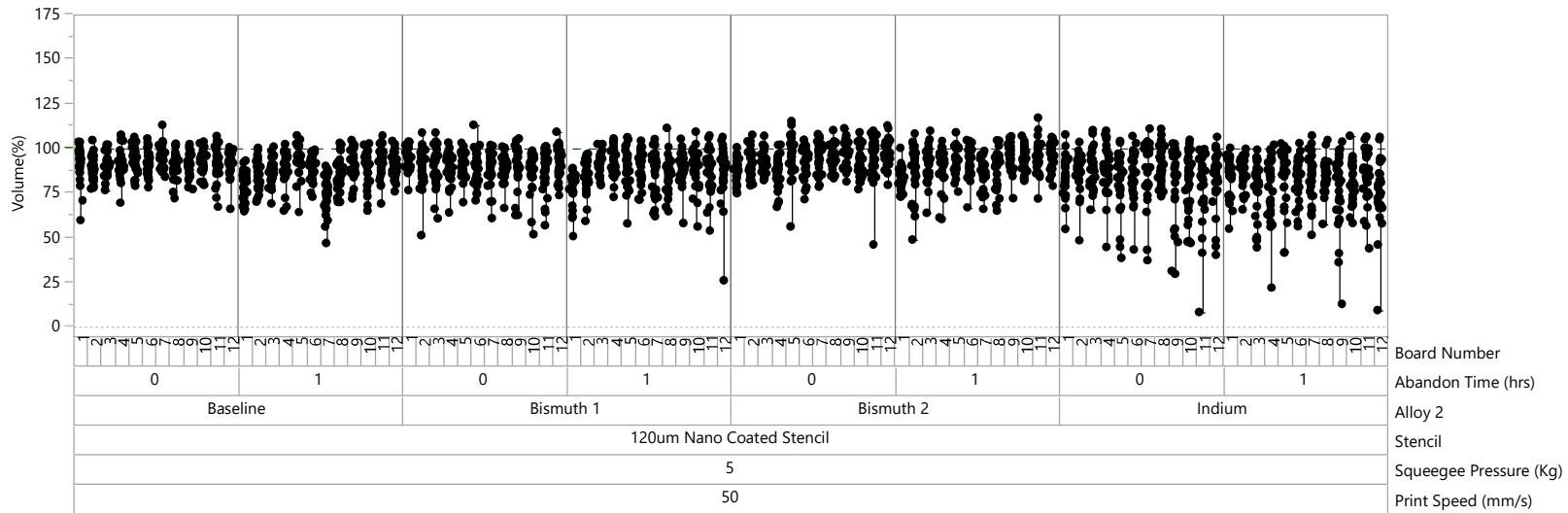
Variability Chart for Volume(%)



Report: Variability Chart

Variability Gauge Component ID=PTF260MS, Size=260x260, Area Ratio=0.542

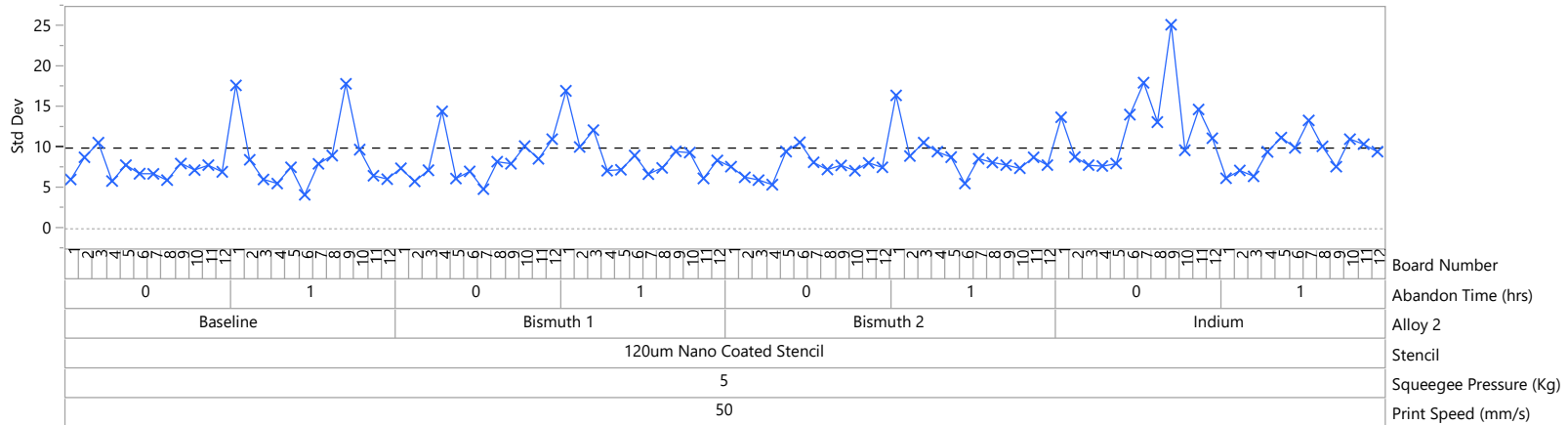
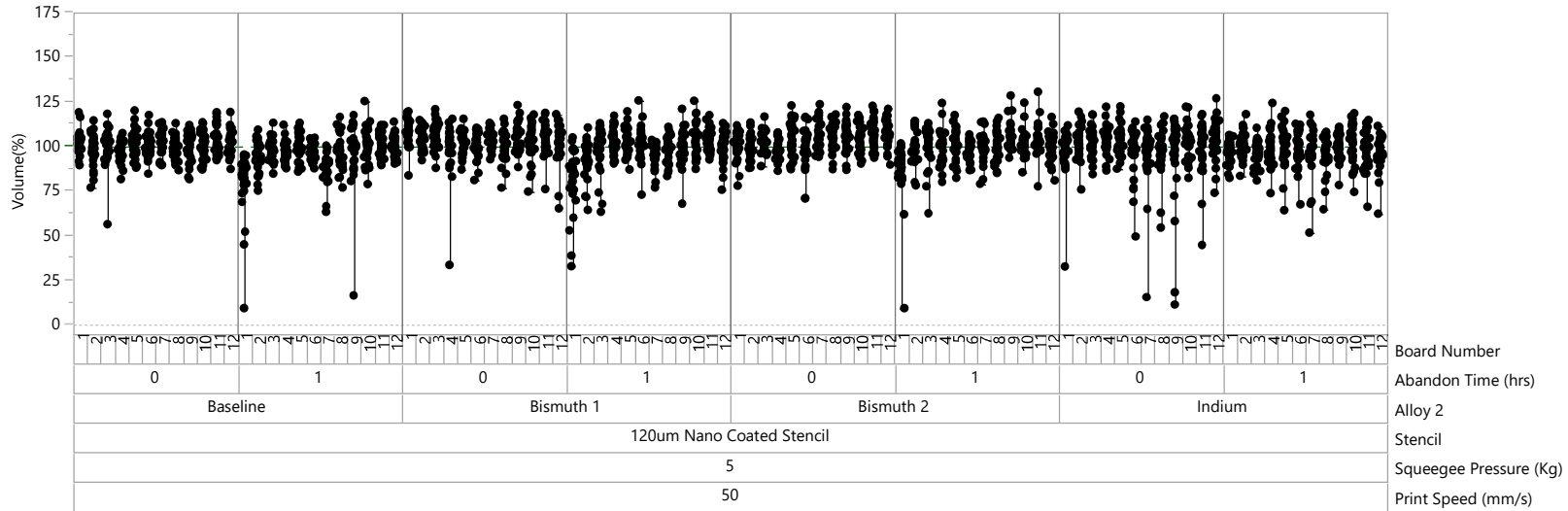
Variability Chart for Volume(%)



Report: Variability Chart

Variability Gauge Component ID=PTF280CC, Size=280x280, Area Ratio=0.583

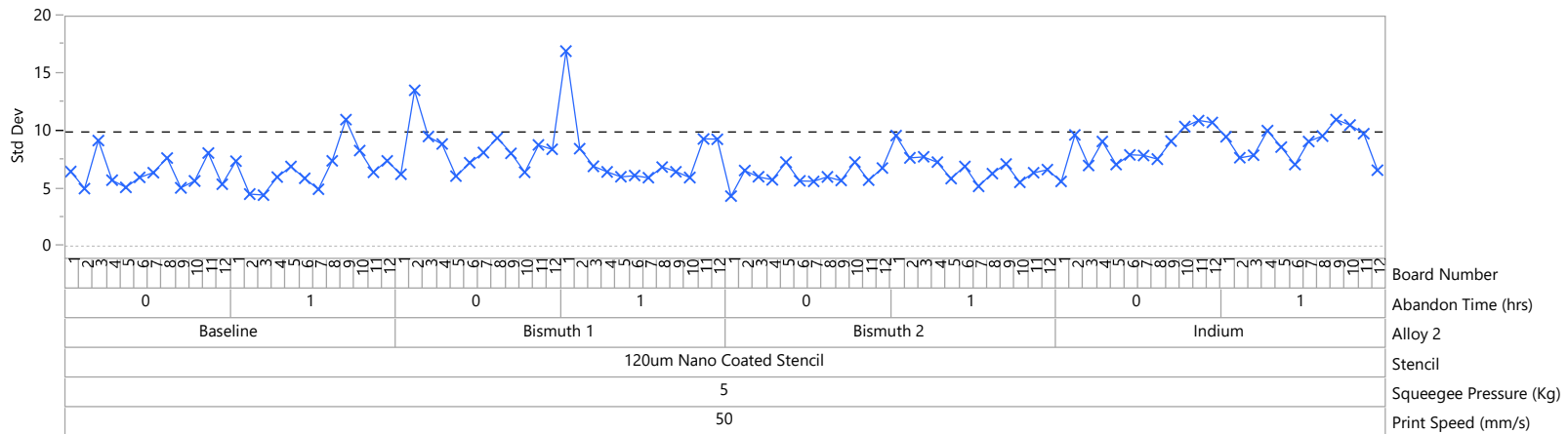
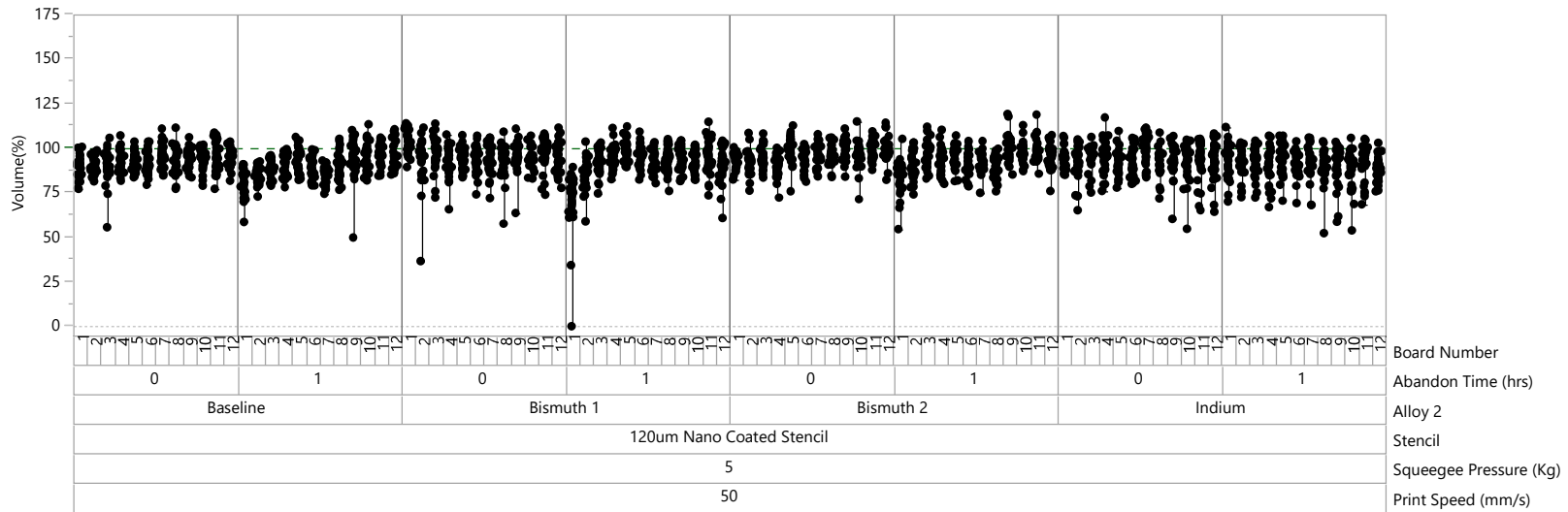
Variability Chart for Volume(%)



Report: Variability Chart

Variability Gauge Component ID=PTF280CS, Size=280x280, Area Ratio=0.583

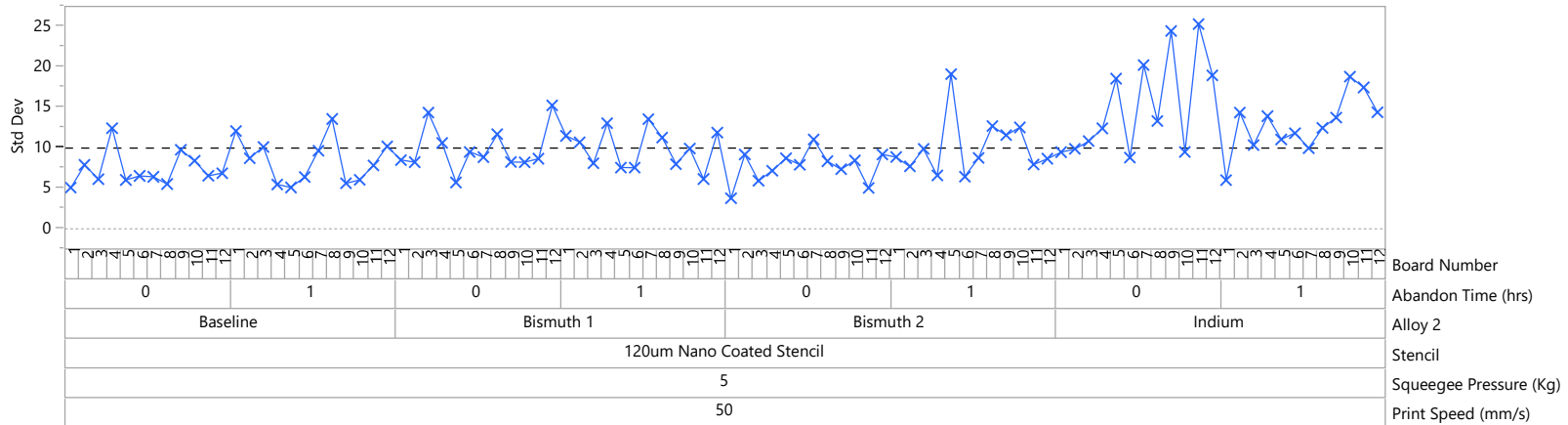
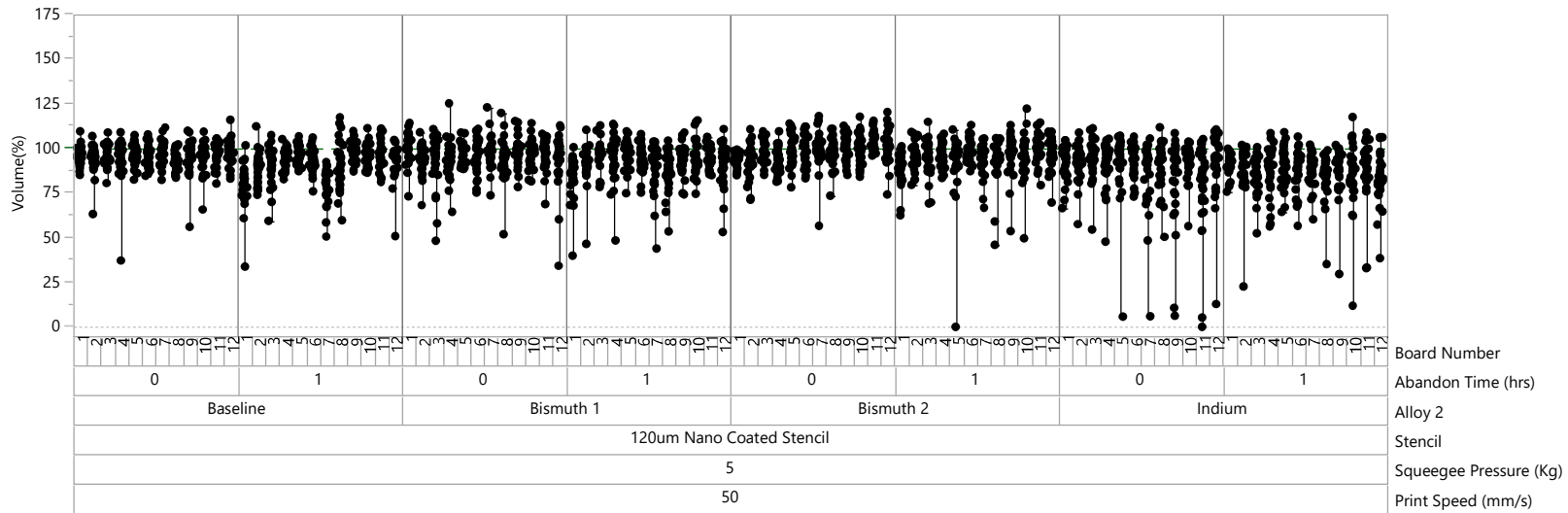
Variability Chart for Volume(%)



Report: Variability Chart

Variability Gauge Component ID=PTF280MC, Size=280x280, Area Ratio=0.583

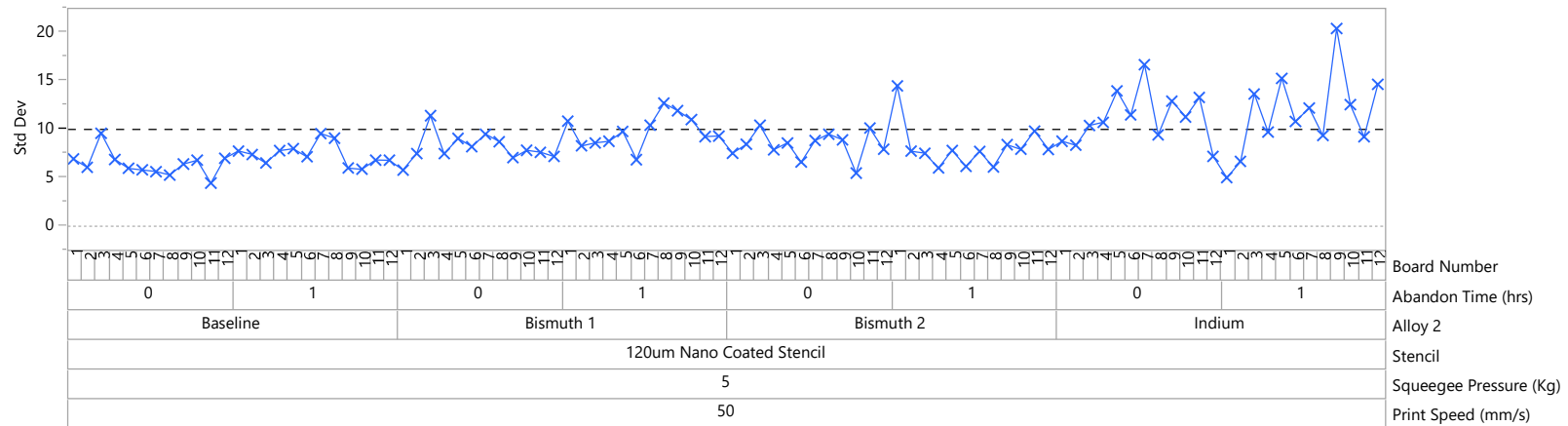
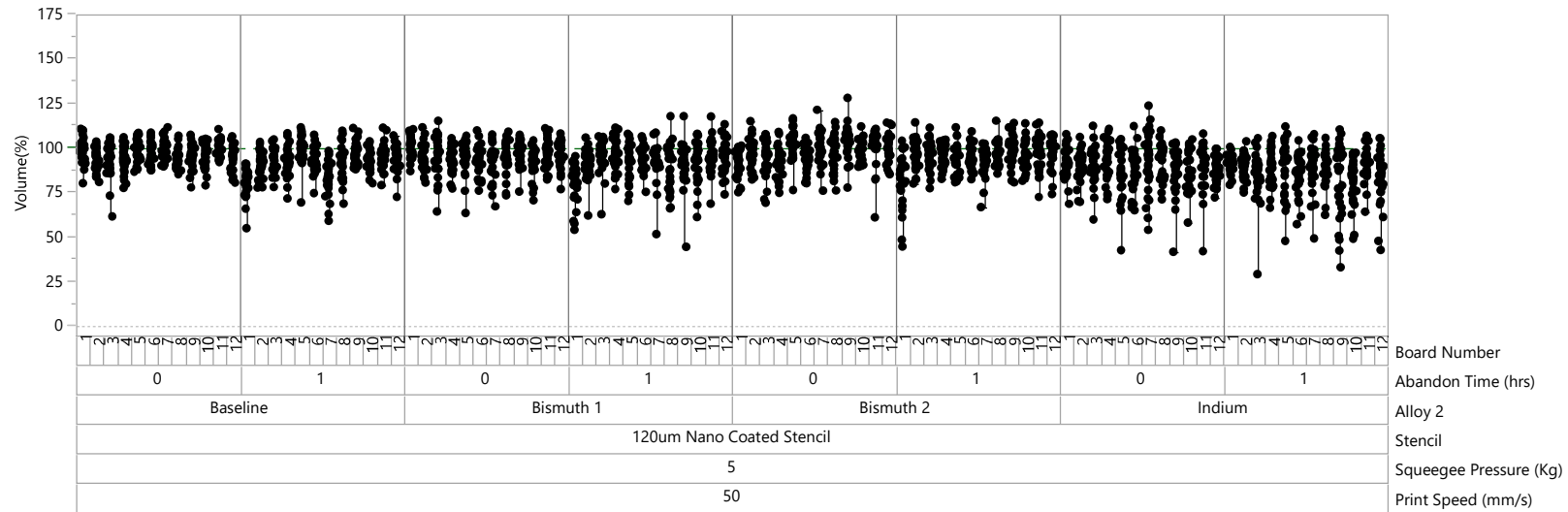
Variability Chart for Volume(%)



Report: Variability Chart

Variability Gauge Component ID=PTF280MS, Size=280x280, Area Ratio=0.583

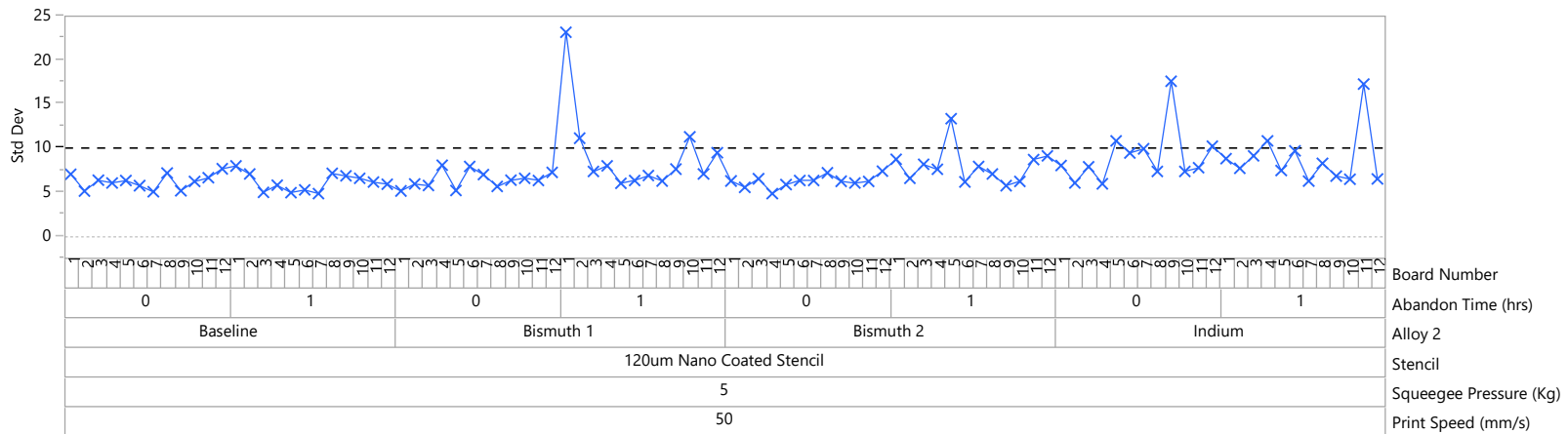
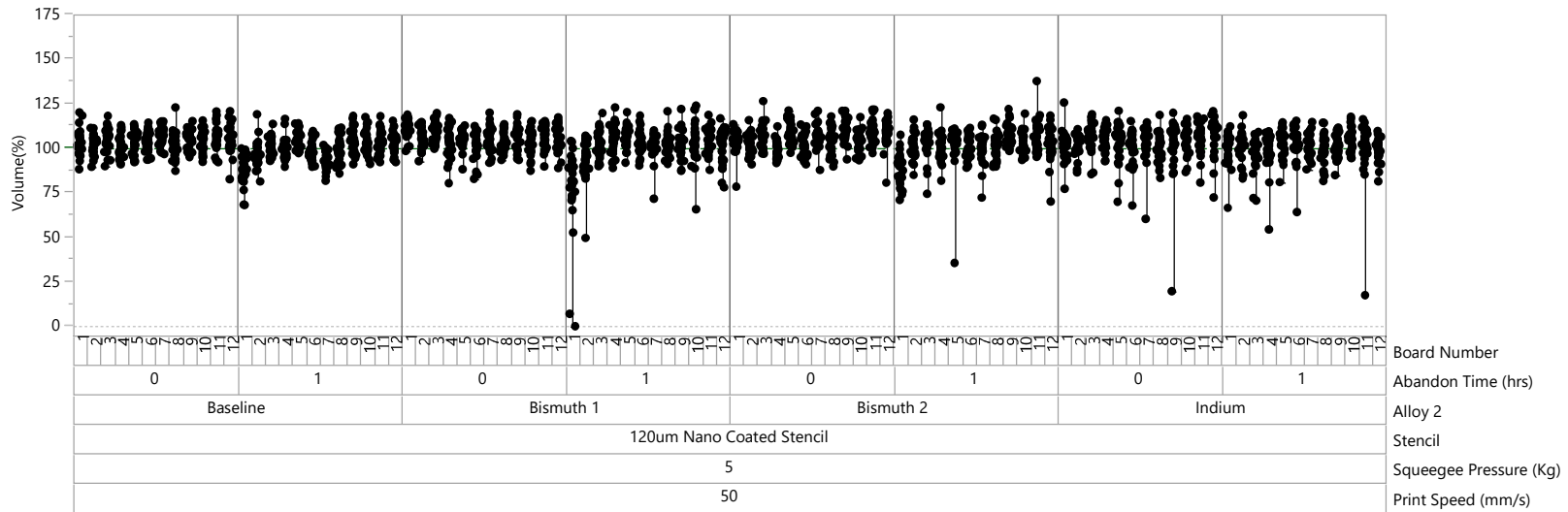
Variability Chart for Volume(%)



Report: Variability Chart

Variability Gauge Component ID=PTF300CC, Size=300x300, Area Ratio=0.625

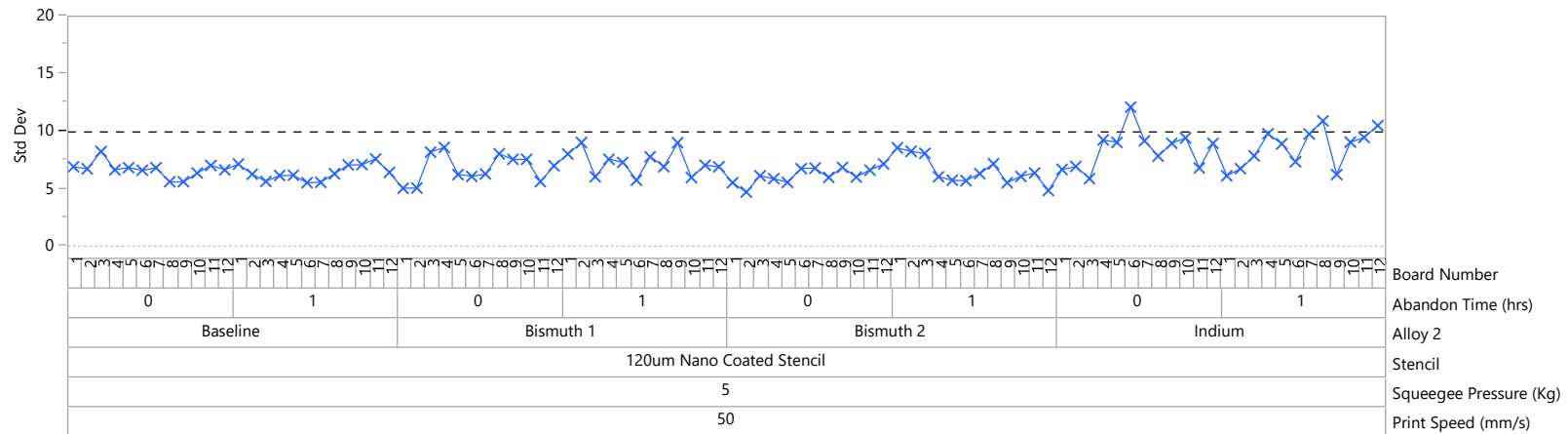
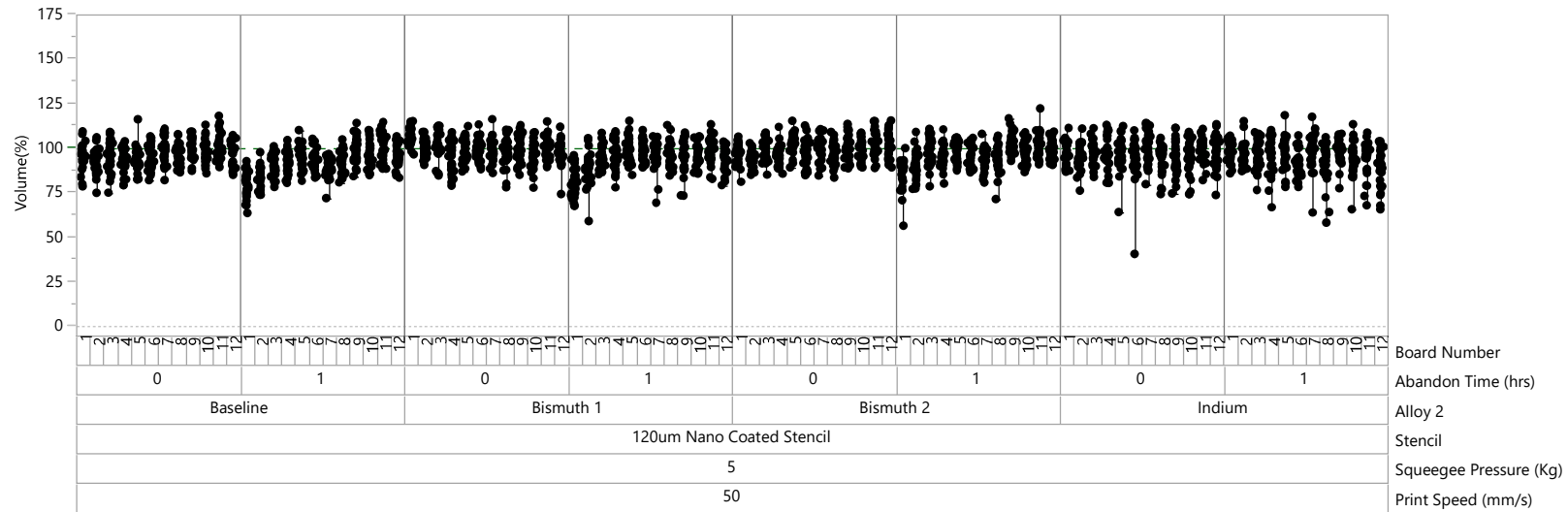
Variability Chart for Volume(%)



Report: Variability Chart

Variability Gauge Component ID=PTF300CS, Size=300x300, Area Ratio=0.625

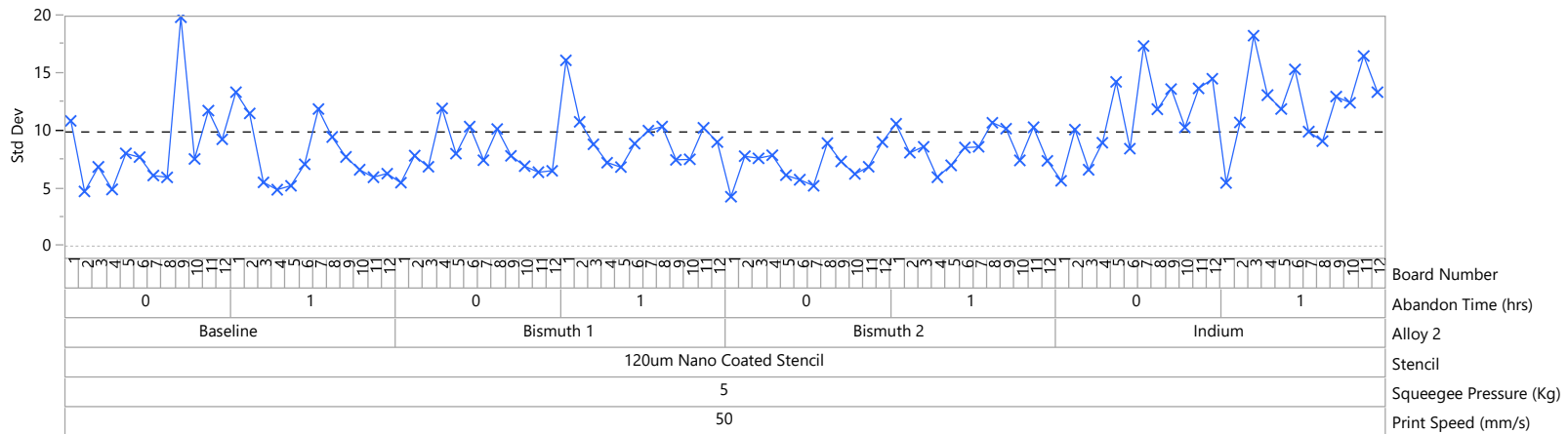
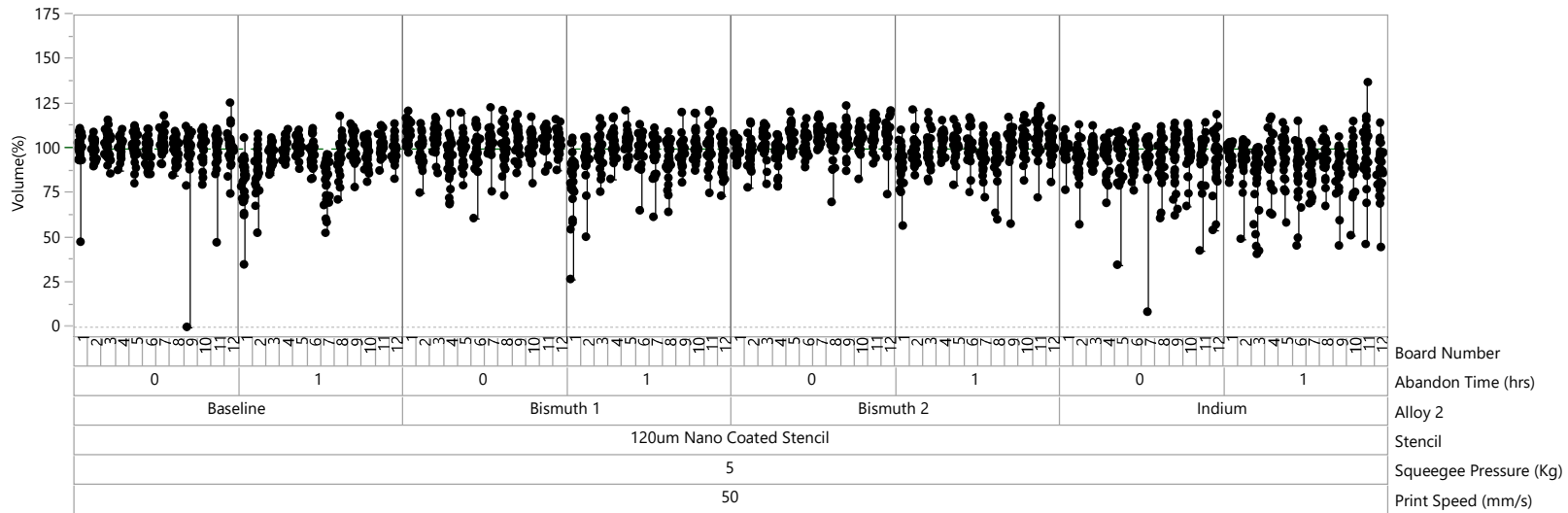
Variability Chart for Volume(%)



Report: Variability Chart

Variability Gauge Component ID=PTF300MC, Size=300x300, Area Ratio=0.625

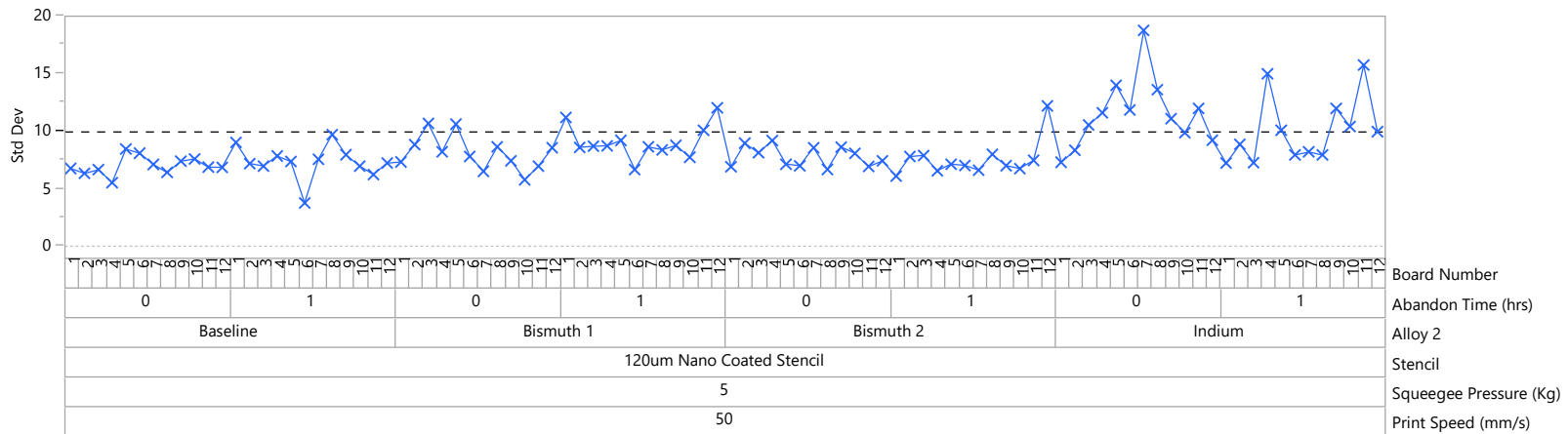
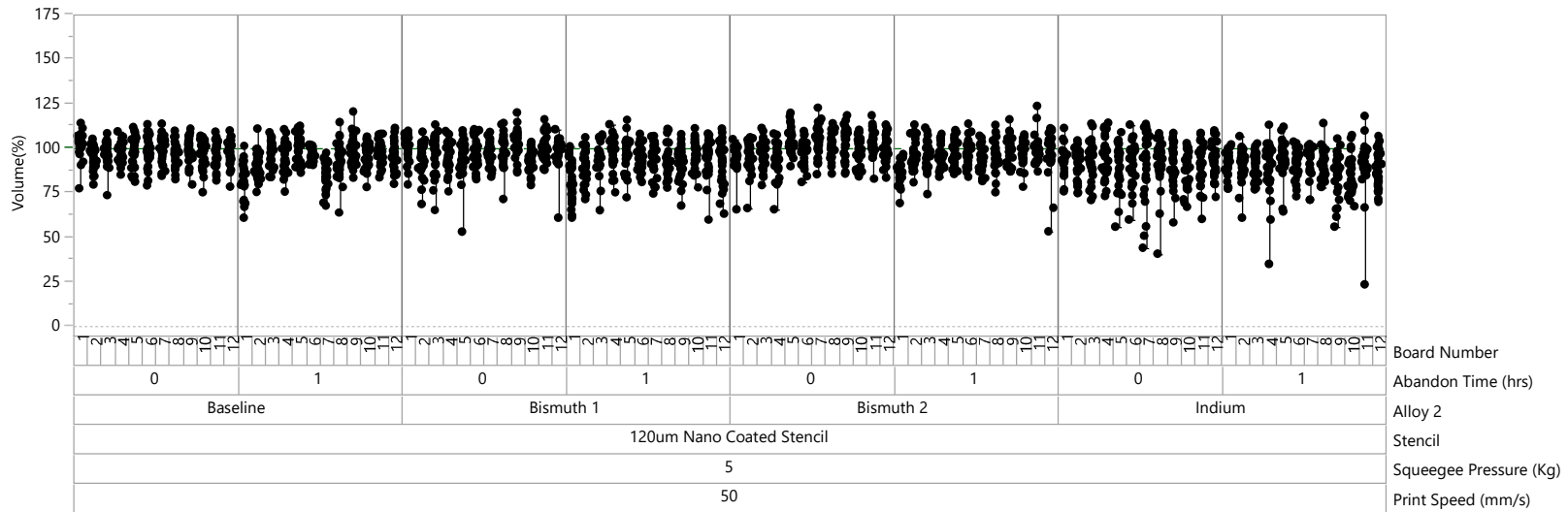
Variability Chart for Volume(%)



Report: Variability Chart

Variability Gauge Component ID=PTF300MS, Size=300x300, Area Ratio=0.625

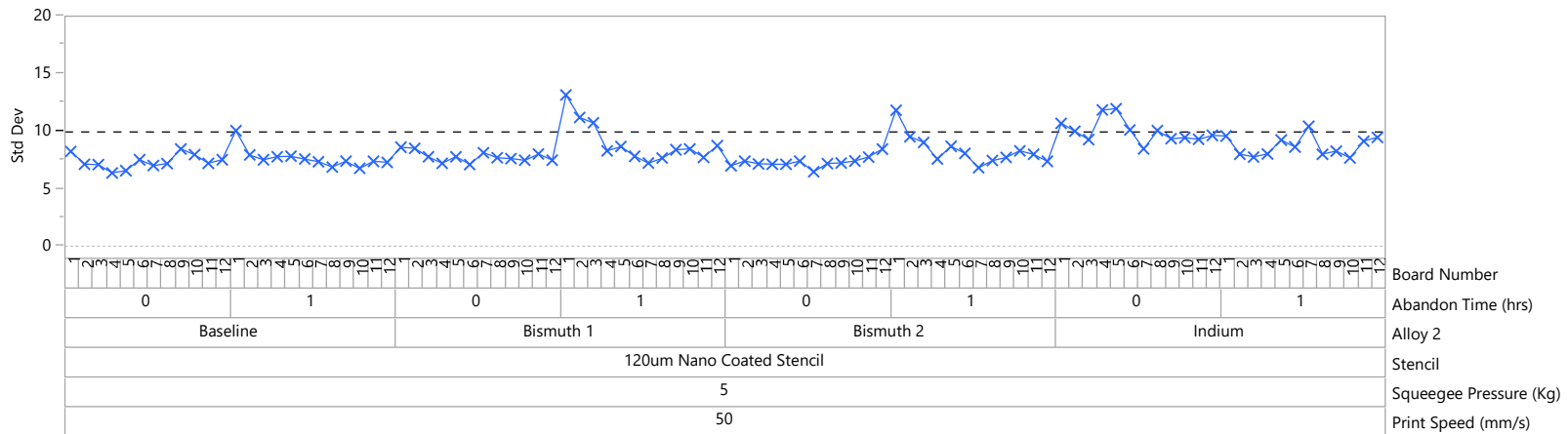
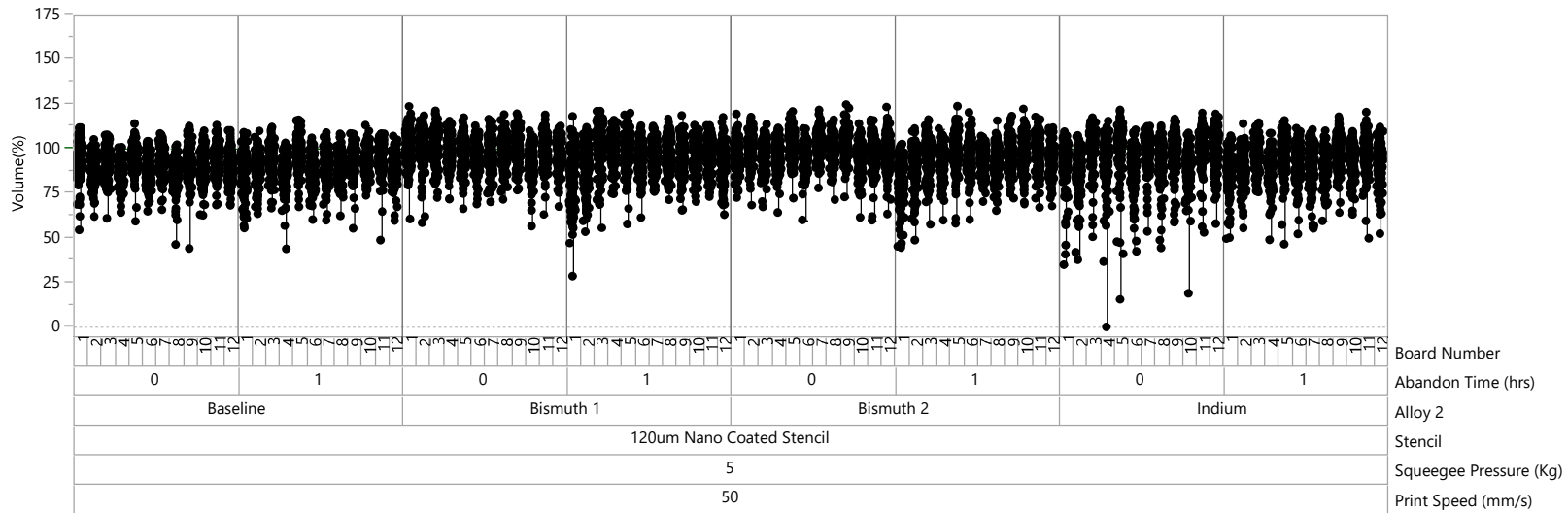
Variability Chart for Volume(%)



Report: Variability Chart

Variability Gauge Component ID=CHP0201C, Size=0.320x0.230, Area Ratio=0.558

Variability Chart for Volume(%)



Report: Variability Chart

Variability Gauge Component ID=CHP0402C, Size=0.900x0.700, Area Ratio=1.64

Variability Chart for Volume(%)

